Petrology, Geochemistry and Geochronology of Kaua'i Lavas over 4·5 Myr: Implications for the Origin of Rejuvenated Volcanism and the Evolution of the Hawaiian Plume

MICHAEL O. GARCIA[1]*, LISA SWINNARD[1], DOMINIQUE WEIS[2], ANDREW R. GREENE[1], TAKA TAGAMI[3], HIROKI SANO[3] AND CHRISTIAN E. GANDY[1]†

[1]DEPARTMENT OF GEOLOGY AND GEOPHYSICS, UNIVERSITY OF HAWAI'I, HONOLULU, HI 96822, USA

[2]PACIFIC CENTRE FOR ISOTOPIC AND GEOCHEMICAL RESEARCH, DEPARTMENT OF EARTH AND OCEAN SCIENCES, UNIVERSITY OF BRITISH COLUMBIA, VANCOUVER, BC, V6T 1Z4 CANADA

[3]DIVISION OF EARTH AND PLANETARY SCIENCES, KYOTO UNIVERSITY, KYOTO 606-8502, JAPAN

Kaua'i lavas provide a unique opportunity to examine over 4·5 Myr of magmatic history at one location along the Hawaiian chain. New field, geochronological, petrological and geochemical results for a large suite of shield, post-shield and rejuvenated lavas are used to examine models for the origin of rejuvenated volcanism, and to evaluate the composition and structure of the Hawaiian plume. Kaua'i has the most voluminous (∼58 km³ based on new field and water well interpretations) and longest-lived suite of rejuvenated lavas (∼2·5 Myr) in Hawai'i. New K–Ar ages and field work reveal an ∼1 Myr gap (3·6–2·6 Ma) in volcanism between post-shield and rejuvenated volcanism. Isotopic and trace element ratios, and modeling of major elements of Kaua'i's rejuvenated lavas require low-degree melting (0·02–2·6%) at ∼1525 ± 10°C and 3·5–4·0 GPa of a heterogeneous, peridotitic plume source. High-precision Pb, Sr, Nd and Hf isotopic, and inductively coupled plasma mass spectrometry trace element data show substantial source variations with a dramatic increase in the depleted component in younger lavas. Some shield, post-shield and rejuvenated lavas (4·3–0·7 Ma) have high $^{208}Pb*/^{206}Pb*$ (radiogenic Pb produced since the formation of the Earth) values (>0·947) indicative of Loa-type compositions, the first reported Loa values in rocks >3 Ma, questioning previous models for the emergence of the Loa component in Hawaiian lavas. The timing, long duration, temporal variation in rock types and voluminous pulse of rejuvenated volcanism (58 km³), and the synchronous eruption of compositionally similar rejuvenated lavas, indicating tapping of common components along 350 km of the Hawaiian chain, are inconsistent with current models for this volcanism. Combining the lithospheric flexure and secondary zone of melting models provides a physical mechanism to initiate and focus the melting at shallower levels within the plume (flexural uplift) with a means to extend the duration of Kōloa volcanism at higher degrees of partial melting.

KEY WORDS: *basalt; geochemistry; Hawaii; Kauai; mantle plume; rejuvenated volcanism*

INTRODUCTION

Rejuvenated volcanism is an enigmatic aspect of hotspot magmatism occurring hundreds of kilometers downstream from the ascending mantle plume stem following an eruptive hiatus of variable duration (∼0·5–2 Myr). Many

*Corresponding author. Telephone: 808-956-6641. Fax: 808-956-5512. E-mail: mogarcia@hawaii.edu
†Present address: US Army Corps of Engineers, Savannah, GA 31401, USA.

oceanic island groups have rejuvenated stage volcanism, including Samoa (Wright & White, 1987), Kerguelen (Weis *et al.*, 1998), the Canary Islands (Hoernle & Schmincke, 1993), Madeira (Geldmacher & Hoernle, 2000), Mauritius (Paul *et al.*, 2005) and Hawai'i (Macdonald *et al.*, 1983). The products of rejuvenated volcanism represent only a tiny fraction (typically ≪1 vol. %) of most oceanic island volcanoes and are generally geochemically distinct from the underlying shield lavas (e.g. Clague & Frey, 1982; Walker, 1990). A depleted source is attributed to most but not all rejuvenated lavas (e.g. Mauritius, Paul *et al.*, 2005). Many geochemical studies have related the depleted source component to the oceanic lithosphere (e.g. Lassiter *et al.*, 2000; Lundstrom *et al.*, 2003; Yang *et al.*, 2003), although other studies have suggested that it is part of the mantle plume that produced the shield stage of volcanism on these oceanic islands (e.g. Maaløe *et al.*, 1992; Geldmacher & Hoernle, 2000; Fekiacova *et al.*, 2007). The latter interpretation is supported by the recognition of a depleted source component in some mantle plume-derived shield stage lavas (e.g. Hawai'i, Iceland, Canaries, Kerguelen, Tahiti and Galápagos), although its origin is widely debated (e.g. Duncan *et al.*, 1994; Hanan *et al.*, 2000; Blichert-Toft & White, 2001; Doucet *et al.*, 2002; Mukhopadhyay *et al.*, 2003; Frey *et al.*, 2005; Geldmacher *et al.*, 2005).

The models currently advocated for the origin of rejuvenated volcanism include: (1) melting of the oceanic lithosphere (e.g. Gurriet, 1987); (2) decompressional melting of the plume as a result of lateral spreading beneath the lithosphere (e.g. Ribe & Christensen, 1999); (3) flexural uplift related to loading the lithosphere above the plume stem (Jackson & Wright, 1970; Bianco *et al.*, 2005). Each model makes predictions about the geochemistry, volume and age of the rejuvenated lavas. The goals of this study are to provide a better understanding of: (1) the source of rejuvenated magmas and the relationship of this source to the Hawaiian plume; (2) the relationship between Hawaiian rejuvenated volcanism and shield volcanism; (3) the mechanisms for generating rejuvenated magmas. To achieve these goals, we have studied the Kōloa Volcanics on Kaua'i, Hawai'i's most voluminous and longest-lived example of rejuvenated volcanism (Fig. 1). A new suite of shield, post-shield and rejuvenated samples was collected for geochronological, petrological, and inductively coupled plasma mass spectrometry (ICP-MS) trace element and radiogenic isotope (Sr, Nd, Pb and Hf) analyses. These results are combined with previous geochemical work on other Kaua'i shield lavas (Mukhopadhyay *et al.*, 2003) to provide the longest (~4·5 Myr) and most comprehensive time-series analysis of volcanism at one location in the Hawaiian chain. The new high-precision isotopic data, especially for Pb and Hf, and the low degrees of partial melting of the Kōloa Volcanics (Maaløe *et al.*, 1992), which

enhance the possibility of sampling source heterogeneities, allow us to better resolve the origin of rejuvenated volcanism and to examine the structure and evolution of the Hawaiian mantle plume.

REGIONAL GEOLOGY

The Hawaiian Islands, the classic example of a mantle plume-produced volcanic chain, have rejuvenated volcanism on six of the older (~6–15 Ma) nine main islands (Ka'ula, Ni'ihau, Kaua'i, O'ahu, Moloka'i and Maui; Fig. 2). Kaua'i, the northernmost and second oldest Hawaiian Island, has the most extensive subaerial deposits of rejuvenated volcanism, covering half of the island (Fig. 1). These deposits, the Kōloa Volcanics, have published ages ranging from 0·375 to 3·65 Ma (McDougall, 1964; Clague & Dalrymple, 1988; Hearty *et al.*, 2005). As discussed below, new field and geochronology studies indicate that Kōloa volcanism probably started at ~2·6 Ma after an ~1 Myr period of quiescence, consistent with the pronounced weathering horizon separating Kōloa from the underlying shield lavas (Stearns, 1946). About 40 Kōloa vents have been identified on the island (Macdonald *et al.*, 1960) and several more were found offshore (Clague *et al.*, 2003; Garcia *et al.*, 2008). The subaerial cones consist of spatter and cinder, although one tuff cone is present (Macdonald *et al.*, 1960). Kōloa lava flows are generally distinct from the underlying shield lavas; they are usually thicker (3–15 vs 1–3 m), mostly 'a'ā to massive flows (rather than pāhoehoe flows), and single flows are commonly separated by weathering horizons or sedimentary deposits. The petrology and geochemistry of Kōloa lavas have been discussed in several studies including those by Macdonald *et al.* (1960), Maaløe *et al.* (1992), Reiners & Nelson (1998), Reiners *et al.* (1999) and Lassiter *et al.* (2000).

Shield lavas and associated fragmental deposits comprise >95 vol. % of Kaua'i. The subaerial shield lavas are known as the Waimea Canyon Basalts (WCB; Macdonald *et al.*, 1960), and are well exposed in the ~1km deep Waimea Canyon and along the north coast of the island (Fig. 1). Tholeiitic shield lavas have K–Ar ages ranging from 5·1 to 4·0 Ma (McDougall, 1979; Clague & Dalrymple, 1988). Rare alkalic lavas (hawaiites and mugearites) are interbedded with and locally cap the tholeiites. These upper WCB flows give K–Ar ages of 3·95–3·87 Ma (McDougall, 1964; Clague & Dalrymple, 1988), representing Kaua'i's post-shield stage of volcanism. WCB lavas have been characterized petrologically and geochemically by several studies including those by Macdonald *et al.* (1960), Feigenson (1984), Maaløe *et al.* (1989) and Mukhopadhyay *et al.* (2003).
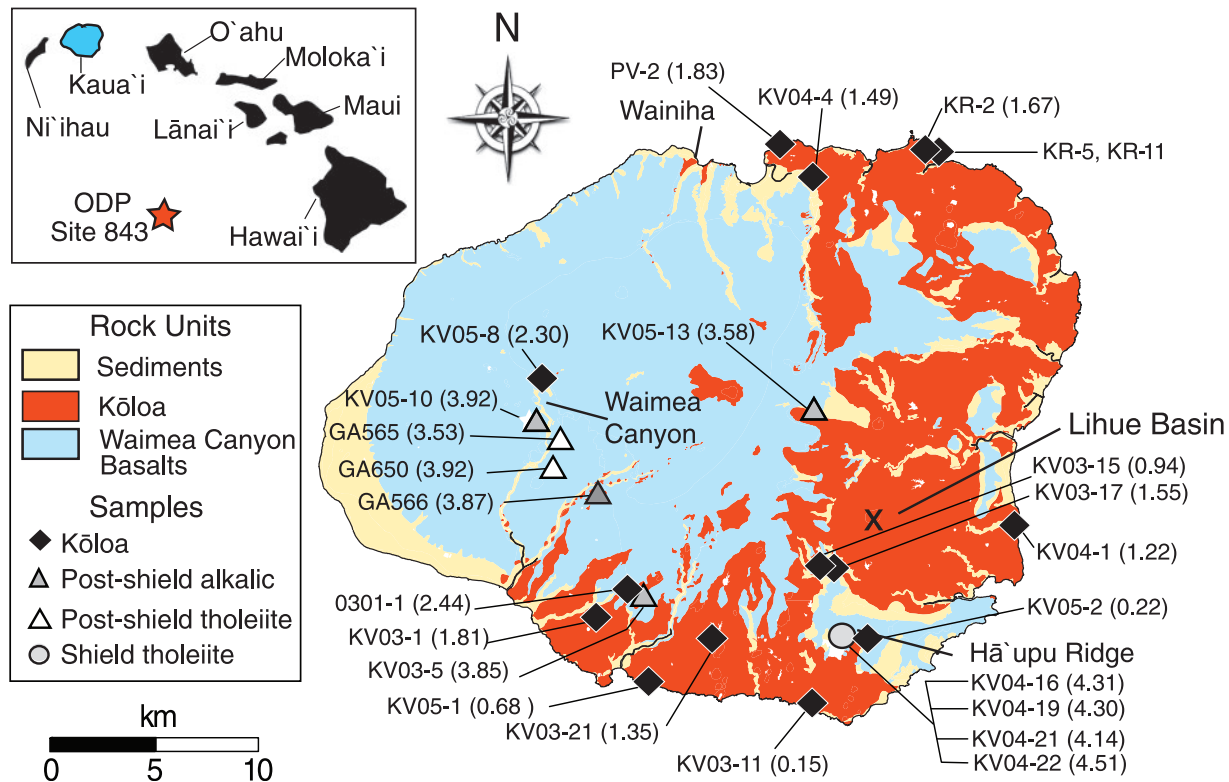
Fig. 1. Geological sketch map of the island of Kaua'i showing the locations and ages (Ma) of isotopically analyzed samples. Sample locations are shown by diamonds for Kōloa Volcanics, triangles for post-shield (3·5–3·9 Ma; open, tholeiitic; gray, alkalic), and a circle for shield samples from the tunnel in Hā'upu Ridge (4·1–4·5 Ma). Other locations noted are Kilohana shield (shown by ×), Lihue Basin and Wainiha gulch. The inset map shows the Hawaiian Islands and the location of the Ocean Drilling Program (ODP) Site 843. The geological map is after Macdonald *et al.* (1960).

VOLUME ESTIMATE FOR KŌLOA VOLCANICS

A quantitative estimate of lava volume is essential for evaluating the origin of rejuvenated volcanism. None were available prior to our study for any sequence of Hawaiian rejuvenated lavas. For Kaua'i, we examined 80 water well logs with rejuvenated lavas (see Electronic Appendix Table 1 for well data, available for downloading at http://www.petrology.oxfordjournals.org/), and measured 41 sections in roadcuts, coastal cliffs and stream gulches where erosion exposed thick sections of Kōloa rocks. These thicknesses (usually a minimum, because the well ended in or outcrop exposed only Kōloa lavas) were compiled onto the Macdonald *et al.* (1960) geological map using ArcMap (GIS) software [Environmental Systems Research Institute (2004); see the Electronic Appendix for methods used]. Volumes in many of the valleys were inferred from isolated residual masses of Kōloa lavas and are considered a minimum. Many of the deeper wells (≥50 m) in the Lihue Basin (Reiners *et al.*, 1999; Izuka, 2006) and the southern coastal areas (Macdonald *et al.*,

1960) were evaluated previously. Other wells were logged by drillers using non-standard terminology. We established the following criteria for distinguishing between shield and rejuvenation lavas in these wells based on our field and petrography work, and that reported by Macdonald *et al.* (1960). Kōloa lavas are thicker than the underlying shield lavas (typically >10 m vs 1–3 m), denser (what drillers called 'blue rock'), have lower vesicularity (usually <10 vol. % vs >10 vol. % for shield lavas), smaller olivine phenocrysts (1–2 mm vs 4–5 mm), and commonly have significant weathering zones or sedimentary deposits between flows (Macdonald *et al.*, 1960). These sedimentary deposits include coralline debris up to 30 m thick (S. Izuka, personal communication, 2004), and breccias with shield and Kōloa lava debris up to 50 m thick in the southern Lihue basin (Macdonald *et al.*, 1960; Reiners *et al.*, 1999). These sedimentary units were excluded in the Kōloa volume estimate. Kōloa lavas extend well beyond the coastline based on examination of coastal sections and water wells near the coast, and recovery of lavas with similar compositions and ages south of Kaua'i (Clague *et al.*, 2003; Garcia *et al.*, 2008). However, the lack of map and thickness data on
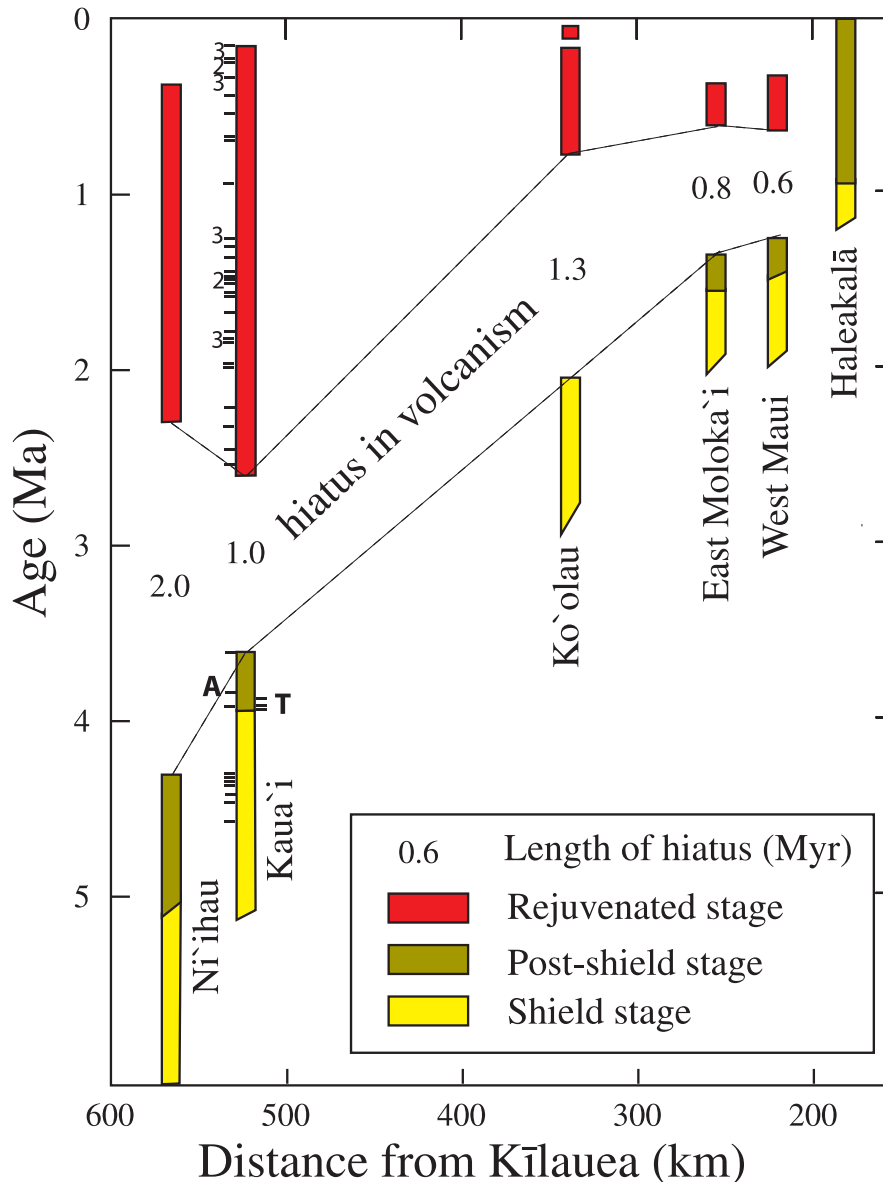
Fig. 2. Plot of age of volcanism vs distance from Kīlauea for the shield, post-shield and rejuvenated stages of Hawaiian volcanoes with rejuvenated volcanism. Distance is measured in kilometers along the chain from Kīlauea volcano. Noteworthy features are the hiatus in volcanism prior to the rejuvenated volcanism and the presence of coeval rejuvenated volcanism from W. Maui to Niʻihau, ∼350 km apart. Figure modified from Ozawa *et al*. (2005) with new ages shown by tick marks on left side of the Kauaʻi column (numbers indicate multiple samples of that age). The new post-shield ages are for alkalic samples (A). Ticks on the right side of the column are for post-shield tholeiites (T) dated by McDougall (1964). These samples were analyzed for major and trace elements and isotopes in our study. See Table 1 for ages.

these submarine lavas necessitated their exclusion from the Kōloa volume estimate. Thus, our volume estimate is a conservative one.

The volume of Kōloa lavas is estimated at 61·5 km³ from our ARC-GIS reconstruction using field work, water well interpretations and the geological map of Macdonald *et al*. (1960). Adjusting this value for the ∼6 vol. % average vesicularity of Kōloa lavas (based on thin-section examination of 85 samples spanning the range of Kōloa rock

types), the dense rock equivalent volume is ∼58 km³. This is the first quantitative volume estimate for a suite of Hawaiian rejuvenated lavas. Compared with the volume of Kauaʻi shield volcano (∼57 600 km³; Robinson & Eakins, 2006), the Kōloa Volcanics represent ∼0·1% of the shield, which is consistent with previous rough estimates for Hawaiian rejuvenated volcanism (e.g. ≪1%; Walker, 1990). The Kōloa Volcanics are the most voluminous Hawaiian example of rejuvenated volcanism

Table 1: K–Ar analytical data from Kaua'i

Sample name	Wt (g)	K₂O (wt %)	$^{40}Ar/^{36}Ar$	$^{38}Ar/^{36}Ar$	$^{40}Ar/^{36}Ar$ initial	$^{40}Ar_{rad}$ (10^{-9} cm³ STP/g)	$^{40}Ar_{air}$ (%)	Calculated age (Ma)	^{36}Ar (10^{-9} cm³ STP/g)	Final age (Ma)
Kāloa Volcanics										
KV03-11	3·20	1·12	312·3 ± 0·6	0·1868 ± 7	295 ± 2	5·3 ± 0·8	94·5	0·15 ± 2	0·31	0·15 ± 0·02
KV03-12	3·74	1·18	331·9 ± 0·7	0·1869 ± 7	296 ± 2	8·3 ± 0·6	89·0	0·219 ± 16	0·23	0·219 ± 0·016
KV05-2	4·37	0·88	308·3 ± 0·6	0·1853 ± 7	291 ± 2	6·3 ± 0·9	94·3	0·22 ± 3	0·36	0·22 ± 0·03
KV05-3	5·84	0·92	320·1 ± 0·6	0·1867 ± 7	295 ± 2	6·8 ± 0·7	92·1	0·23 ± 2	0·27	0·23 ± 0·02
KV03-6	1·49	1·25	336·8 ± 0·8	0·1782 ± 14	295·5*	9·1 ± 0·2	87·7	0·227 ± 5	0·22	0·227 ± 0·005
KV03-8	5·99	1·07	354·2 ± 0·7	0·1876 ± 9	298 ± 3	11·1 ± 0·6	84·1	0·32 ± 2	0·20	0·320 ± 0·018
KV03-10	1·59	0·82	304·7 ± 0·6	0·1866 ± 9	295 ± 3	8·6 ± 2·5	96·7	0·32 ± 9	0·84	0·32 ± 0·09
KV03-7	1·48	0·91	350·5 ± 0·9	0·0613 ± 23	295·5*	9·5 ± 1·7	84·3	0·324 ± 7	0·17	0·324 ± 0·007
KV05-14	5·11	1·17	403·8 ± 0·8	0·1874 ± 9	297 ± 3	15·8 ± 0·5	73·5	0·419 ± 14	0·15	0·419 ± 0·014
KV03-27	2·10	0·73	325·7 ± 0·7	0·1873 ± 7	297 ± 2	12·2 ± 1·1	91·1	0·52 ± 5	0·42	0·52 ± 0·05
KV05-1	3·63	1·02	374·4 ± 0·7	0·1856 ± 8	291 ± 3	22·2 ± 0·8	77·9	0·68 ± 2	0·27	0·68 ± 0·02
KR-3	3·80	1·28	365·4 ± 0·7	0·1878 ± 8	298 ± 2	28·4 ± 1·1	81·6	0·69 ± 3	0·42	0·69 ± 0·03
KV03-15	2·86	1·22	387·3 ± 0·8	0·1865 ± 7	294 ± 2	37·1 ± 1·1	76·0	0·94 ± 3	0·40	0·94 ± 0·03
KV03-20	0·74	1·02	411·7 ± 0·8	0·1876 ± 8	298 ± 2	39·3 ± 1·0	72·3	1·19 ± 3	0·34	w.m.
	2·24	1·02	461·7 ± 0·9	0·1862 ± 9	294 ± 3	40·8 ± 0·9	63·6	1·24 ± 3	0·24	1·22 ± 0·02
KV04-1	1·49	0·77	339·0 ± 0·7	0·1856 ± 7	291 ± 2	30·4 ± 1·6	86·0	1·22 ± 7	0·64	1·22 ± 0·07
KV04-13	5·91	0·88	441·2 ± 0·9	0·1867 ± 7	295 ± 2	34·7 ± 0·7	66·8	1·22 ± 3	0·24	1·22 ± 0·03
KV04-9	4·52	1·10	408·8 ± 0·8	0·1867 ± 7	295 ± 2	45·8 ± 1·1	72·1	1·29 ± 3	0·40	1·29 ± 0·03
KV03-21	0·73	1·46	460·4 ± 0·9	0·1864 ± 7	294 ± 2	65·3 ± 1·2	63·9	1·39 ± 3	0·39	w.m.
	1·50	1·46	686·8 ± 1·5	0·1872 ± 10	296 ± 3	62·3 ± 0·8	43·2	1·33 ± 2	0·16	1·35 ± 0·02
KV04-8	2·26	1·01	447·4 ± 0·9	0·1858 ± 7	292 ± 2	46·7 ± 0·9	65·3	1·44 ± 3	0·30	1·44 ± 0·03
KV04-3	2·94	1·11	527·0 ± 1·1	0·1872 ± 7	296 ± 2	52·4 ± 0·8	56·3	1·46 ± 3	0·23	1·46 ± 0·03
KV03-18	2·25	1·06	510·3 ± 1·0	0·1850 ± 7	290 ± 2	50·0 ± 0·8	56·8	1·46 ± 3	0·23	1·46 ± 0·03
KV03-19	2·22	0·92	548·3 ± 1·1	0·1854 ± 7	291 ± 2	43·6 ± 0·6	53·1	1·47 ± 3	0·17	1·47 ± 0·03
KV04-4	2·99	1·24	638·1 ± 1·3	0·1871 ± 7	296 ± 2	59·7 ± 0·7	46·4	1·49 ± 2	0·17	1·49 ± 0·02
KV03-17	2·99	1·12	544·1 ± 1·1	0·1851 ± 7	290 ± 2	56·1 ± 0·8	53·3	1·55 ± 3	0·22	1·55 ± 0·03
KV05-15	0·63	1·65	416·1 ± 0·8	0·1887 ± 10	301 ± 3	84 ± 3	72·4	1·57 ± 5	0·73	1·57 ± 0·05
KR-2	2·99	0·50	339·4 ± 0·7	0·1879 ± 8	299 ± 2	27·2 ± 1·7	88·0	1·68 ± 11	0·67	w.m.
	1·50	0·50	332·8 ± 0·7	0·1874 ± 7	297 ± 2	27·0 ± 1·9	89·2	1·66 ± 12	0·75	1·67 ± 0·08
0301-4	3·00	1·71	563·3 ± 1·1	0·1877 ± 8	298 ± 2	96·4 ± 1·3	52·9	1·75 ± 3	0·36	1·75 ± 0·03
KV03-1	1·22	1·58	346·2 ± 0·7	0·1870 ± 7	296 ± 2	90 ± 5	85·4	1·76 ± 9	1·78	w.m.
	1·51	1·58	347·0 ± 0·7	0·1865 ± 7	294 ± 2	95 ± 5	84·8	1·85 ± 9	1·79	1·81 ± 0·07
PV-2	4·36	0·96	666·5 ± 1·3	0·1860 ± 9	293 ± 3	56·5 ± 0·7	43·9	1·83 ± 3	0·15	1·83 ± 0·03
KV03-4	3·15	1·81	511·8 ± 1·0	0·1870 ± 7	296 ± 2	106·7 ± 1·6	57·8	1·83 ± 3	0·49	1·83 ± 0·03
KV03-3	1·50	1·59	375·7 ± 0·8	0·1864 ± 7	294 ± 2	97 ± 3	78·2	1·89 ± 6	1·19	w.m.
	1·29	1·59	374·4 ± 0·7	0·1871 ± 7	296 ± 2	90 ± 3	79·1	1·76 ± 6	1·16	1·83 ± 0·04
KV04-10	3·67	0·96	472·9 ± 0·9	0·1877 ± 8	298 ± 2	61·0 ± 1·1	63·0	1·97 ± 4	0·35	1·97 ± 0·04
KV03-2	1·20	1·41	359·5 ± 0·7	0·1874 ± 7	297 ± 2	87 ± 4	82·6	1·92 ± 8	1·40	w.m.
	1·48	1·41	355·1 ± 0·7	0·1864 ± 7	294 ± 2	94 ± 4	82·8	2·06 ± 9	1·53	1·99 ± 0·06
KV05-16	2·80	1·08	528·2 ± 1·1	0·1877 ± 8	298 ± 2	73·3 ± 1·1	56·4	2·10 ± 4	0·32	2·10 ± 0·04
KV05-8	4·41	1·16	796·2 ± 1·6	0·1866 ± 7	294 ± 2	86·1 ± 1·0	37·0	2·30 ± 3	0·17	2·30 ± 0·03
0301-1	2·24	1·20	507·3 ± 1·0	0·1871 ± 7	296 ± 2	94·5 ± 1·5	58·4	2·44 ± 5	0·45	2·44 ± 0·05
KV04-6	2·25	0·98	833·6 ± 1·7	0·1883 ± 10	300 ± 3	79·8 ± 0·9	35·9	2·52 ± 4	0·15	2·52 ± 0·04

(continued)

Table 1: Continued

Sample name	Wt (g)	K$_2$O (wt %)	^{40}Ar/^{36}Ar	^{38}Ar/^{36}Ar	^{40}Ar/^{36}Ar initial	^{40}Ar$_{rad}$ (10^{-9} cm^3 STP/g)	^{40}Ar$_{air}$ (%)	Calculated age (Ma)	^{36}Ar (10^{-9} cm^3 STP/g)	Final age (Ma)
Post-shield										
KV05-13	2·13	1·42	768·7 ± 1·5	0·1863 ± 7	294 ± 2	163·6 ± 1·9	38·2	3·58 ± 5	0·34	3·58 ± 0·05
KV03-5	2·92	1·10	756·4 ± 3	0·1859 ± 7	292 ± 2	136·4 ± 1·6	38·7	3·85 ± 66	0·29	3·85 ± 0·06
KV05-10	2·92	0·92	860·3 ± 1·7	0·1874 ± 8	297 ± 3	116·2 ± 1·3	34·5	3·92 ± 6	0·21	3·92 ± 0·06
Shield: Hā'upu Tunnel										
KV04-16	0·76	0·58	346·6 ± 0·7	0·1883 ± 8	300 ± 2	82 ± 5	86·5	4·38 ± 2	1·75	w.m.
	0·64	0·58	347·4 ± 0·7	0·1881 ± 8	299 ± 2	80 ± 4	86·1	4·26 ± 2	1·65	4·31 ± 0·17
KV04-17	0·64	0·36	336·3 ± 0·7	0·1858 ± 7	292 ± 2	51 ± 3	86·9	4·36 ± 3	1·15	w.m.
	1·41	0·36	336·7 ± 0·7	0·1860 ± 7	293 ± 2	51 ± 3	86·9	4·36 ± 3	1·16	4·36 ± 0·18
KV04-19	0·64	0·49	367·7 ± 0·7	0·1853 ± 7	291 ± 2	71 ± 2	79·0	4·52 ± 16	0·92	w.m.
	1·43	0·49	372·0 ± 0·7	0·1867 ± 7	295 ± 2	64 ± 2	79·3	4·11 ± 15	0·84	4·30 ± 0·11
KV04-24	0·69	0·33	322·8 ± 0·6	0·1855 ± 7	291 ± 2	46 ± 4	90·2	4·30 ± 35	1·46	w.m.
	0·70	0·33	323·6 ± 0·6	0·1850 ± 8	290 ± 3	50 ± 4	89·5	4·64 ± 36	1·47	4·46 ± 0·25
Other shield										
KV05-7	2·89	0·41	395·2 ± 0·8	0·1867 ± 7	295 ± 2	58·1 ± 1·6	74·6	4·35 ± 13	0·58	4·35 ± 0·13
KV05-17	1·36	0·43	345·8 ± 0·7	0·1873 ± 7	297 ± 2	62 ± 3	85·8	4·43 ± 24	1·27	4·43 ± 0·24
KV05-9	4·35	0·35	595·2 ± 1·2	0·1850 ± 11	290 ± 4	52 ± 8	48·7	4·57 ± 8	0·17	4·57 ± 0·08

Isotopic abundance and decay constants for ^{40}K are $\lambda_e = 0.581 \times 10^{-10}$ a^{-1}, $\lambda_\beta = 4.962 \times 10^{-10}$ a^{-1} and ^{40}K/K $= 1.167 \times 10^{-4}$ (Steiger & Jäger, 1977). Analytical errors are 1σ. Sample name with suffix p indicates that only preliminary Ar analysis was performed on the sample. No mass fractionation correction is applied to KV03-6p and KV03-7p, which have ^{40}Ar/^{36}Ar initial ratio of 295·5 ± 0·0 because of low output of ^{38}Ar. ^{36}Ar concentrations are without errors. Only samples suitable for further discussion have final ages. w.m., weighted mean from two ages.

(Macdonald *et al.*, 1983). Thus, on other Hawaiian Islands, rejuvenated volcanism represents ≪0·1 vol. % of the total island.

SAMPLES AND ANALYTICAL TECHNIQUES

Kōloa samples were chosen from a new suite of 129 rocks collected during an extensive field program. Thin-section analysis of these samples identified 72 unaltered to weakly altered samples (minor iddingsite on olivine, and no calcite and zeolites in vesicles) for X-ray fluorescence (XRF) analysis. Thirty-seven of the freshest Kōloa samples (see Electronic Appendix Table 2 for locations of these and other samples) were chosen for unspiked K–Ar dating, the preferred method for dating young samples with high atmospheric contamination (Matsumoto *et al.*, 1989). Fifteen samples, all but one K–Ar dated, were selected for ICP-MS trace element, and Pb, Sr, Nd and Hf isotopic analyses to cover the age (2·44–0·15 Ma), compositional (weakly alkalic to foidite), and spatial ranges for the Kōloa Volcanics (Fig. 1). The undated sample was collected and analyzed twice (KR-5 and -11) because of its unusual chemistry. Attempts to date it were unsuccessful.

Stratigraphically, it is one of the oldest Kōloa samples. In addition, seven shield and seven post-shield samples were chosen for comparison with the Kōloa lavas. Four of the post-shield samples were previously K–Ar dated but were otherwise uncharacterized samples (GA prefix; McDougall, 1964). Four of the shield samples (two dikes and two flows) are from a tunnel into the Hā'upu Ridge (SE side of the island; Fig. 1).

Geochronology work was performed at Kyoto University starting with 80–100 g of rock crushed in a stainless steel pestle. Samples were sieved to 250–500 μm, and washed with deionized water and then acetone in an ultrasonic bath. Phenocrysts and xenoliths were carefully removed from all samples using a Frantz isodynamic separator to minimize the presence of extraneous argon. Argon isotope ratios were measured using a VG Isotech© VG3600 mass spectrometer operated in the static mode, connected to extraction and purification lines. Sensitivity of the mass spectrometer was determined by analyzing a known amount of the air standard, which was generally ~1·2 × 10^7 V/cm^3 STP. Mass discrimination in the mass spectrometer was corrected assuming ^{40}Ar/^{36}Ar and ^{38}Ar/^{36}Ar ratios of the air standard to be 295·5 and 0·1869, respectively (Matsumoto & Kobayashi, 1995). With

Table 2: XRF major and trace element compositions of Kōloa, post-shield and shield Kauaʻi lavas

Stage:	Kāloa Volcanics							
Sample:	KV03-11	KV05-2	KV05-1	KV03-15	KV04-1	KV03-21	KV04-4	KV03-17
Rock type:	AB	B	B	F	AB	B	B	B
Age (Ma):	0·15 ± 0·02	0·22 ± 0·03	0·68 ± 0·02	0·94 ± 0·03	1·22 ± 0·07	1·35 ± 0·02	1·49 ± 0·02	1·55 ± 0·03
SiO_2	45·01	44·06	41·16	40·14	46·82	44·17	44·22	42·10
TiO_2	2·483	2·206	2·947	2·892	1·630	2·702	2·112	2·320
Al_2O_3	12·97	11·79	10·75	9·76	11·45	12·04	11·66	10·89
Fe_2O_3	13·07	13·32	14·02	14·01	12·79	13·44	13·55	13·98
MnO	0·19	0·20	0·20	0·22	0·18	0·19	0·20	0·20
MgO	8·82	12·27	13·24	15·25	13·64	11·11	13·08	13·51
CaO	12·56	11·11	12·50	12·47	10·15	11·91	11·26	11·54
Na_2O	3·23	3·18	3·14	3·18	2·58	2·41	2·65	3·46
K_2O	1·020	0·998	0·854	1·133	0·580	1·195	0·890	1·132
P_2O_5	0·449	0·391	0·647	0·634	0·251	0·542	0·390	0·527
Total	99·80	99·53	99·46	99·69	100·07	99·71	100·01	99·66
Mg-no.	59·8	67·0	67·5	70·6	70·1	64·5	68·0	68·0
LOI	0·04	−0·37	2·15	0·74	0·41	1·70	0·19	−0·55
V	283	267	267	303	207	261	262	281
Ni	169	324	422	413	505	291	348	370
Cr	330	529	722	648	698	437	575	594
Zn	113	113	108	122	107	125	115	120
Rb	26·1	24·8	25·0	32·8	13·4	28·8	22·5	28·5
Sr	638	548	702	790	404	751	560	686
Y	23·0	20·3	23·2	20·6	25·0	31·0	19·9	20·4
Zr	119	125	203	168	85	169	112	139
Nb	41·1	40·3	67·5	63·4	23·2	54·5	39·5	52·2

Stage:	Kāloa Volcanics						
Sample:	KR-2	KV03-1	PV-2	KV05-8	0301-1	KR-5	KR-11
Rock type:	F	F	AB	F	B	F	F
Age (Ma)	1·67 ± 0·08	1·81 ± 0·07	1·83 ± 0·03	2·30 ± 0·03	2·44 ± 0·05	—	—
SiO_2	40·26	39·48	45·34	40·84	43·67	38·15	37·92
TiO_2	3·320	3·544	2·002	3·306	2·550	3·467	3·473
Al_2O_3	10·07	9·54	12·45	10·83	11·42	9·31	9·29
Fe_2O_3	14·34	15·28	13·21	14·24	13·68	15·33	15·46
MnO	0·20	0·20	0·20	0·20	0·19	0·21	0·23
MgO	14·27	13·38	11·04	13·11	12·38	15·04	14·20
CaO	12·71	12·02	11·57	12·41	11·32	13·24	13·31
Na_2O	3·56	3·33	2·46	2·55	3·08	3·11	3·31
K_2O	0·523	1·674	0·705	1·187	1·118	1·028	1·455
P_2O_5	0·690	0·696	0·497	0·531	0·443	0·960	0·920
Total	99·94	99·14	99·47	99·20	99·85	99·84	99·57
Mg-no.	68·7	65·9	64·8	67·0	66·6	68·4	66·9
LOI	1·36	0·59	0·21	1·03	0·09	1·29	0·98
V	270	315	235	336	286	323	315
Ni	331	387	275	354	314	329	315
Cr	528	539	431	664	526	493	466
Zn	111	144	113	113	112	135	140
Rb	10·4	39·2	16·6	38·8	24·4	27·1	31·4
Sr	802	761	629	653	601	1085	1176
Y	22·0	23·6	27·9	19·9	22·5	25·4	27·1
Zr	203	252	125	182	164	292	302
Nb	69·1	73·5	36·3	61·5	42·8	88·4	91·5

(continued)

1513

Table 2: Continued

Stage:	Post-shield						Shield			
Sample:	KV05-13	KV03-5	GA 566	GA 565	GA 650	KV05-10	KV04-21	KV04-19	KV04-16	KV04-22
Rock type:	B	B	Haw	Thol	Thol	B	Thol	Thol	Thol	Thol
Age (Ma):	3·58 ± 0·05	3·85 ± 0·06	3·87 ± 0·04	3·9	3·92 ± 0·03	3·92 ± 0·06	4·14 ± 0·20	4·30 ± 0·11	4·31 ± 0·17	4·51 ± 0·07
SiO_2	43·91	44·06	50·33	50·41	49·51	44·09	51·02	50·40	47·40	50·12
TiO_2	4·138	2·619	3·279	2·375	2·581	2·667	2·402	2·369	2·147	2·278
Al_2O_3	15·98	11·93	20·84	13·44	13·63	12·67	13·13	12·75	10·05	12·44
Fe_2O_3	13·78	14·09	13·89	12·67	12·81	13·84	12·31	11·96	12·83	12·33
MnO	0·21	0·19	0·17	0·18	0·18	0·19	0·17	0·17	0·17	0·17
MgO	5·59	12·18	1·77	7·71	7·73	11·17	8·01	9·89	17·54	10·49
CaO	9·04	10·51	2·51	10·54	10·56	10·91	10·04	9·70	7·48	9·65
Na_2O	4·57	2·65	3·56	2·44	2·41	3·36	2·26	2·20	1·73	2·01
K_2O	1·448	0·889	2·315	0·374	0·234	0·906	0·484	0·426	0·376	0·438
P_2O_5	0·701	0·449	1·332	0·233	0·237	0·472	0·264	0·261	0·261	0·238
Total	99·37	99·57	100·00	100·37	99·88	100·28	100·09	100·12	99·99	100·16
Mg-no.	47·2	65·6	21·9	57·3	57·1	64·0	58·9	64·5	75·1	65·2
LOI	0·08	0·03	6·60	0·36	0·33	−0·30	−0·11	−0·06	−0·20	−0·10
V	233	290	140	242	245	291	263	247	207	259
Ni	12	359	17	107	123	295	114	245	818	287
Cr	0	638	10	323	326	575	358	558	939	632
Zn	123	119	137	106	109	109	115	113	128	116
Rb	30·8	20·4	45·3	6·5	1·7	22·1	8·7	7·0	5·7	7·0
Sr	1203	661	608	310	330	661	316	317	317	312
Y	31·0	27·1	105·5	25·3	25·8	32·8	23·7	19·0	19·0	22·4
Zr	200	151	543	143	146	139	139	137	137	129
Nb	58·0	35·0	79·3	14·7	13·7	34·3	12·7	13·2	13·2	14·0

Samples listed from oldest to youngest except two undated samples. Ages: GA series from McDougall (1964), adjusted to newer age constants, except for GA 565 (see text for explanation); other samples from Table 1. Major element concentrations are in wt %; trace element concentrations in ppm. Thol, tholeiite; Haw, hawaiite; AB, alkali basalt; B, basanite; F, foidite based on total alkalis–silica diagram (Fig. 3). Mg-number calculated assuming 90% of total iron is ferrous. (See text for methods used.) LOI, loss-on-ignition. Negative LOI values indicate oxidation of sample during fusion to convert all iron to Fe_2O_3.

this procedure, the initial $^{40}Ar/^{36}Ar$ is calculated from measured $^{38}Ar/^{36}Ar$ assuming mass-dependent isotopic fractionation during rock formation. The air standard was analyzed every 2–3 samples each day and a hot blank was measured every 5–10 samples. SORI93 biotite was used for calibration of the air standard. Blank levels were less than $1·7 \times 10^{-8} cm^3$ STP for mass 40. No peak drift was observed during analyses. Errors for ^{40}Ar, $^{40}Ar/^{36}Ar$ and $^{38}Ar/^{36}Ar$ were estimated from multiple analyses of the air standard, and were 2·0%, 0·2–0·4% and 0·4–0·8%, respectively. For measurement of potassium content, a flame emission spectrometer Asahi Rika FP-33D was used in a peak integration mode with a lithium internal standard. Analytical error for potassium measurement is ∼2%,

estimated from standard deviation of multiple analyses of standard JB3 and JA2. Additional information on methods has been given by Ozawa *et al.* (2005).

Microprobe analyses of olivine were undertaken using a five-spectrometer JEOL 8500F instrument operating at 20 kV and 200 nA with a 10 μm beam and 30 s counting times for Mg, Fe and Si, and 60 s for Ni, Mn and Ca using natural standards. Analytical error was <0·1% for Fo and ∼0·01 wt % for CaO, MnO and NiO based on replicate analyses of San Carlos and Marjalati olivine standards. For whole-rock geochemical work, samples were coarsely crushed (1–8 mm) with a tungsten-carbide (WC) coated hydraulic press, ultrasonically cleaned in Millipore water and dried for 24 h at 70°C, and hand-picked to

remove fragments with signs of alteration. This procedure ensured that only the freshest parts of each sample were analyzed. The efficiency of this process is reflected by the relatively low loss-on-ignition (LOI) values (for methods, see Rhodes, 1996) for most samples (<1·0 wt %) compared with previous studies. The clean rock fragments were split into two aliquots; one for XRF, and the other for ICP-MS and isotopes. Samples for XRF analysis were powdered using WC-lined mills and analyzed for major and trace elements at the University of Massachusetts (for analytical procedures and precision see Rhodes, 1996; Rhodes & Vollinger, 2004). For the ICP-MS trace element analysis, samples were powdered in an agate mill, digested in concentrated sub-boiled HF and HNO_3 for 48 h, and then redigested in 6N sub-boiled HCl for 24 h. Once dried, they were re-dissolved in concentrated HNO_3, dried down again and diluted 5000 times using a 10 ppb In, 1% HNO_3 solution. The trace elements were analyzed by high-resolution ICP-MS using a Finnigan Element2 system at the Pacific Centre for Isotopic and Geochemical Research (PCIGR) at the University of British Columbia (Pretorius *et al.*, 2006). For the isotopic analyses, the agate powdered samples were extensively acid-leached with 6N HCl using methods outlined by Weis & Frey (1991, 1996), Weis *et al.* (2005) and Nobre Silva *et al.* (2009) to remove any post-eruptive alteration (7–18 steps, average 10 to reach clear solution, with weigh losses of 23–89%, average 67%). After a 48 h period of digestion in concentrated sub-boiled HF and HNO_3 and a 24 h period of digestion in 6N sub-boiled HCl, the samples were purified using Pb, Sr, Nd and Hf anionic exchange columns to separate these elements (for detailed procedure see Connelly *et al.*, 2006; Weis *et al.*, 2006, 2007). The lab blanks measured during the course of this study were <50 pg for Pb, ~100 pg for Sr and Nd, and 30 pg for Hf (i.e. entirely negligible in comparison with the amount of these elements in the analysed samples). The Pb and Hf isotopes were analyzed by multi-collector ICP-MS using a Nu Plasma system and the Sr and Nd isotopes were analyzed by thermal ionization mass spectrometry (TIMS) using a Finnigan Triton system, both at the PCIGR.

During this study, the NBS 987 standard gave $^{87}Sr/^{86}Sr = 0.710253 \pm 13$ ($n = 7$); La Jolla Nd: $^{143}Nd/^{144}Nd = 0.511853 \pm 11$ ($n = 11$); JMC 475: $^{176}Hf/^{177}Hf = 0.282154 \pm 29$ ($n = 13$), and SRM 981: $^{206}Pb/^{204}Pb = 16.9425 \pm 17$, $^{207}Pb/^{204}Pb = 15.5002 \pm 21$, $^{208}Pb/^{204}Pb = 36.7222 \pm 60$ ($n = 20$). The BHVO-2 USGS standard was analyzed together with the samples and the results are within error of the published values (Weis *et al.*, 2006, 2007). Complete procedural duplicates were analyzed for one Kōloa and one post-shield sample, yielding an external reproducibility for the isotope ratios of Pb ($^{206}Pb/^{204}Pb$, $^{207}Pb/^{204}Pb$, $^{208}Pb/^{204}Pb$) of 264, 278 and 226 ppm, and for Sr, Nd and Hf of 18, 17 and 32 ppm, respectively.

GEOCHRONOLOGY OF KAUA'I LAVAS

Here we present a comprehensive geochronological examination of the longest duration of volcanism on any Hawaiian Island (Fig. 2). Forty-seven Kaua'i samples (37 Kōloa, three post-shield and seven shield lavas) were successfully analyzed by the unspiked K–Ar method (^{36}Ar contents $<2.5 \times 10^{-9}$ cm^3 STP/g; Table 1). Ten samples were run in duplicate with all but one shield sample agreeing within analytical error (Table 1). Nine samples are from the same flows previously analyzed using conventional K–Ar (Clague & Dalrymple, 1988) or Ar–Ar methods (Hearty *et al.*, 2005). Our new ages are within analytical error of the previous ages.

The new Kōloa ages more than double the number of ages for this rock group and extend the age range to more recent times (0·15 Ma vs a previous age of 0·375 Ma; Hearty *et al.*, 2005; Fig. 2). The seven youngest ages (0·15–0·32 Ma; Table 1) are from a cluster of cones and associated flows on the south coast of Kaua'i that were identified by Macdonald *et al.* (1960) as the youngest volcanic features on the island (Fig. 1; ages are plotted for only those samples analyzed for isotopes). There is no other geographical pattern to the age distribution of Kōloa flows (Fig. 1). The six flows with ages of 0·5–1·0 Ma are widely distributed across the island (Fig. 1) from the SW (KV05-01, 0·68 Ma) to NE (KR-3, 0·69 Ma). Sample KR-3 is from a dike that cuts the only identified tuff cone complex on Kaua'i (tuff cones are common in the other major Hawaiian rejuvenated complexes on the islands of O'ahu and Ni'ihau; Stearns & Vaksvik, 1935; Stearns, 1947). This dike fed a flow that is separated from the tuff cone by an ~1 m thick red weathering horizon. A juvenile block from the tuff cone (KR-2) yielded a 1·67 Ma age, suggesting the weathering horizon formed over ~1 Myr.

Twenty of the new Kōloa ages are 1–2 Ma for flows widely scattered across the island (Fig. 1). The previously undated, largest (10 km × 14 km) Hawaiian rejuvenated cone, Kilohana on the SE flank of Kaua'i (Fig. 1), was formed during this interval (five ages ranging from 1·22 to 1·55 Ma). Older Kōloa samples (>2·0 Ma) are rare, and were found along the north coast, in deep canyons in the center and on the SW flank of the island (Fig. 1), as was noted by Clague & Dalrymple (1988). The oldest new age is 2·52 Ma, which is much younger than the oldest reported Kōloa age of 3·65 ± 0·03 Ma age for a basanitic flow overlying a conglomerate (Clague & Dalrymple, 1988). We also dated this basanite flow, obtaining an age of 3·92 ± 0·06 Ma (Table 1). Both ages are within the range for post-shield Kaua'i lavas (3·6–3·9 Ma; McDougall,

1964; Table 1). Some post-shield alkalic and rejuvenated lavas are nearly indistinguishable in major and trace elements, and isotopes, so rock composition is not a valid indicator of whether this flow is from the rejuvenated stage (see major element section below). Furthermore, there is a gap of $\sim$1 Myr between this age and the next youngest dated Kōloa sample (2·59 Ma; Clague & Dalrymple, 1988), despite systematic sampling of Kōloa lavas during this and previous geochronological studies (55 dated samples; McDougall, 1964; Clague & Dalrymple, 1988; Hearty et al., 2005; Table 1). We conclude that Kōloa volcanism began at $\sim$2·6 Ma and its duration was $\sim$2·45 Myr (Fig. 2).

Utilizing our new volume estimate of 58 km^3 and the 2·45 Myr age span for the Kōloa Volcanics, the average magma flux rate was $\sim$24 km^3/Myr. This is probably the highest average flux rate of rejuvenated volcanism on any Hawaiian island (Macdonald et al., 1983; Sherrod et al., 2007). Melting models for rejuventated volcanism generally predict Gaussian magma production rates (Ribe & Christensen, 1999; Bianco et al., 2005). Thus, Kōloa maximum magma flux rates were probably much higher than 24 km^3/Myr, much higher than for any other Hawaiian sequence of rejuvenated lavas but much lower than during post-shield (5000 km^3/Myr) or shield stages (50 000 km^3/Myr; Walker, 1990).

Ages were obtained for three new post-shield samples: two basanites (3·85 and 3·92 Ma) and a hawaiite (3·58 Ma) from the central and southern parts of the island (Fig. 1; Table 1). These ages are nearly identical to the previously reported K–Ar ages for samples considered as post-shield (McDougall, 1964; Clague & Dalrymple, 1988). One previously analyzed tholeiitic sample (GA 565) has an anomalously young age (3·53 Ma) for its stratigraphic position (between two other tholeiitic flows with ages of 3·92 and 3·87 Ma; McDougall, 1964); thus, its age is assumed to be $\sim$3·9 Ma. Combining the new and previous geochronology results indicates that the age gap between the end of shield volcanism and onset of rejuvenated volcanism on Kaua'i is $\sim$1·0 Myr (Fig. 2). Kaua'i's gap is intermediate between the longer hiatuses reported for Ko'olau (1·3 Myr; Ozawa et al., 2005) and Ni'ihau ($\sim$2·0 Myr; Sherrod et al., 2007) and the shorter time gaps for much lower volume rejuvenated volcanism complexes on Moloka'i (0·8 Myr; Clague et al., 1982) and West Maui (0·6 Myr; Tagami et al., 2003). These gaps are somewhat shorter than the reported gaps in the Canary Islands (3–4 Myr; e.g. Hoernle & Schimincke, 1993).

Seven new shield lava samples were successfully dated yielding ages of 4·30–4·57 Ma (Table 1). Four of the new ages are from the tunnel section through Hā'upu Ridge, a previous undated feature on the SE flank of Kaua'i (Fig. 1). Averaging the Hā'upu ages yields 4·36 ± 0·08 Ma, identical to the average of eight ages from two areas on the north flank of Kaua'i (4·35 ± 0·09 Ma) but significantly younger than the average of eight ages for the SW flank of Kaua'i (5·1 ±0·2 Ma; McDougall, 1979). Two new samples (a dike and a flow at river level) from Waimea Canyon, an area previously undated and considered a younger part of Kaua'i's shield (Macdonald et al., 1960), gave ages of 4·35 and 4·43 Ma. These ages are nearly identical to many of the ages for the northern flanks of the Kaua'i shield (4·35 Ma; McDougall, 1979). Another sample from a north shore canyon (Wainiha; Fig. 1) gave the oldest age, 4·57 Ma. The combined suite of new and previous ages (25) shows that much of the subaerially exposed Kaua'i shield formed between 4·6 and 4·3 Ma, indicating that growth during this period was relatively rapid. During this time interval, the adjacent shield volcano on the island of Ni'ihau was dying (its youngest age is 4·3 Ma; 13 other ages are 4·7–5·6 Ma; Sherrod et al., 2007).

In summary, combining our new geochronology results with those from previous studies indicates that the Kaua'i subaerial shield-building stage was active from >5·1 to 4·0 Ma, followed by post-shield tholeiitic and alkalic lavas from 3·95 to 3·6 Ma. After a gap in volcanism of $\sim$1 Myr, rejuvenated stage volcanism started at 2·6 Ma and continued to 0·15 Ma.

PETROGRAPHY AND OLIVINE CHEMISTRY OF KAUA'I LAVAS

The Kōloa lavas are olivine-phyric alkali basalts. The samples examined here typically have intergranular to subophitic textures with variable amounts of olivine and rare ($\leq$2 vol. %) clinopyroxene (cpx), plagioclase or melilite phenocrysts (0·5 mm) and sparse vesicles (average 6 vol. %) in a groundmass of cpx with variable amounts of olivine, plagioclase (or melilite), nepheline, Fe–Ti oxides, apatite, cryptocrystalline material, glass, and phlogopite (only in two samples). Olivine is the most common phenocryst ($<$1−14 vol. %) and is usually euhedral, although some crystals show disequilibrium or deformation features (embayments or kink bands) and are xenocrysts. Partial alteration of olivine to iddingsite is widespread, although it is usually restricted to crystal rims ($<$0·01 mm) in our samples. Chromite inclusions are common in olivine. Subhedral to euhedral, concentrically zoned clinopyroxene (cpx, usually augite, rarely titanaugite) occurs in 15% of the samples. Euhedral plagioclase or melilite, and subhedral nepheline are present in $<$5% of the samples. Microphenocrysts (0·1−0·5 mm) of these minerals are more common. Olivine is found in all of the samples (1−18 vol. %), cpx in half of the samples ($<$1−13 vol. %), plagioclase in 60%

of the samples (<1–17 vol. % but not in the foidite samples), melilite (<1–12 vol. % in 10% of the samples and only the foidites), nepheline (1–6 vol. % in foidites), and Fe–Ti oxides (<1–6 vol. %) in many samples. Ultramafic xenoliths (mostly dunite) were found in ∼5% of Kōloa rocks [for a description of Kōloa xenoliths see Ross *et al.* (1954) and White (1966)]. The extent of alteration of the Kōloa lavas is highly variable from weak to intense. In general, the younger samples, especially those from the drier southern coast, are less altered. Secondary minerals in the Kōloa lavas include iddingsite after olivine, clay replacement of glassy and cryptocrystalline material, and zeolites and calcite in vesicles.

The analyzed post-shield lavas range from aphyric hawaiite to strongly olivine-phyric alkali basalt (up to 10 vol. % olivine), all with sparse vesicles (1–5 vol. %) in a holocrystalline matrix. Two samples have plagioclase microphenocrysts and one of these, KV03-05, has ∼1 vol. % cpx phenocrysts and rare, small (1 cm) harzburgite xenoliths. These rocks are unaltered or have thin iddingsite rims on olivine. The 11 examined shield lavas range from aphyric to picritic (10–15 vol. % olivine) basalts, although most samples have <5 vol. % total olivine. Several samples have elongate or xenocrystic olivine. Plagioclase and cpx phenocrysts and microphenocrysts are rare in these shield lavas, consistent with their relatively high MgO content (7·5–10·2 wt %). Most of the lavas are holocrystalline (a few are cryptocrystalline) and fresh, especially those from the tunnel, although some have thin iddingsite rims on olivine. Vesicularity is highly variable in this suite, <1–30 vol. %.

The forsterite content (Fo) of olivine in 55 crystals from nine Kōloa lavas varies from 87·9 to 67·9% for rocks with Mg-number $(100[Mg/(Mg + Fe^{2+})])$ of 62·4–71·7. Olivine cores range from 83 to 88% Fo, somewhat lower than previously published values for Kōloa samples (Fo 86–89; Maaløe *et al.*, 1992). Most olivine are unzoned or normally zoned, although reversed zoning was found in seven lower Fo crystals in four samples. Olivine in rocks with Mg-numbers >68 are too low in Fo to be in equilibrium with the whole-rock magma composition. NiO contents range from 0·14 to 0·41 wt %. There is a good correlation of Ni with Fo for almost all olivines within each Kōloa sample, unlike in Gran Canaria lavas, which were interpreted to have crystallized from multiple batches of magma (Gurenko *et al.*, 2010). CaO varies greatly, 0·14–0·74 wt % (most values are 0·21–0·39 wt %), generally increasing with decreasing Fo, although the lowest CaO contents are in reversely zoned, low-Fo crystals. These moderate to high CaO contents are indicative of crustal-level crystallization (e.g. Larsen & Pederson, 2000). The olivine compositions of Kauaʻi shield tholeiites have been well characterized

by Maaløe *et al.* (1989), so no new samples were analyzed in this study.

MAJOR AND TRACE ELEMENT COMPOSITIONS OF KAUAʻI LAVAS

The Kōloa, post-shield and shield lavas show wide major element ranges (Table 2, Electronic Appendix Table 3). The relatively low LOI values, generally <1·4 wt % for Kōloa and <0·6 wt % for all but one of the shield and post-shield samples, indicate that the major element ranges of variation are probably not related to alteration. Low LOI values confirm the petrographic observation that the samples selected for geochemical analysis are unaltered to weakly altered. The Kōloa samples have alkali basalt to foidite compositions (Fig. 3). The post-shield stage lavas are tholeiites, basanites and a hawaiite (Fig. 3), typical of post-shield lavas on other Hawaiian volcanoes (e.g. Spengler & Garcia, 1988; Frey *et al.*, 1991). The shield lavas are exclusively tholeiites (Fig. 3), as noted by previous studies (e.g. Mukhopadhyay *et al.*, 2003).

The Kōloa lavas from this study show comparable major element concentrations and ranges to those previously reported for some oxides (e.g. MgO vs SiO_2), although somewhat higher CaO/Al_2O_3 and K_2O (Fig. 4). The higher CaO/Al_2O_3 for some new samples and the positive trend of this ratio with MgO for samples with >10 wt % MgO (Fig. 4c) is probably indicative of variable degrees of partial melting (higher ratio, lower degree) rather than cpx fractionation because these rocks have few or no cpx phenocrysts and there is an inverse correlation of Sc content with MgO (opposite to what is expected for cpx fractionation; Tables 2 and 3). The same interpretation was invoked to explain the MgO variation trends for Honolulu rejuvenated lavas (Clague & Frey, 1982). The lower K_2O of some previously reported samples is probably related to alteration (LOI values up to 10 wt %; e.g. Reiners & Nelson, 1998). Most of the new Kōloa samples have relatively high MgO (11–15 wt %), Mg-numbers (70·6–64·5), and Ni (275–505 ppm) and Cr contents (431–722 ppm; Table 2), similar to other Hawaiian rejuvenated lavas (e.g. Honolulu Volcanics; Clague & Frey, 1982). No correlation was found between olivine phenocryst abundance and MgO content in Kōloa lavas with MgO contents <15 wt % that we and Maaløe *et al.* (1992) examined. Thus, the composition of most Kōloa lavas with MgO of 13–15 wt % is probably indicative of their near primary magma composition rather than olivine accumulation, which is consistent with the forsterite contents of the olivine in many of these lavas (86–89%; Maaløe *et al.*, 1992).

The Kōloa Volcanics are strongly enriched in incompatible elements (Tables 2 and 3; Figs 4 and 5; Electronic

Table 3: ICP-MS trace element compositions of Kōloa, post-shield and shield Kauaʻi lavas

Stage:	Kāloa Volcanics						
Sample:	KV03-11	KV05-2	KV05-1	KV03-15	KV04-1	KV03-21	KV04-4
Li	6·11	5·42	5·09	6·82	4·66	6·33	5·40
Sc	27·1	25·4	25·3	23·4	24·4	22·9	25·3
Sb	0·01	0·02	0·00	0·05	0·00	0·03	0·03
Cs	0·13	0·27	0·20	0·55	0·15	0·27	0·32
Ba	478	431	438	601	295	663	431
Ta	2·06	2·21	2·09	3·96	0·97	2·94	2·42
Th	3·11	2·90	2·88	4·70	1·96	4·46	3·22
U	0·61	0·72	0·70	1·16	0·52	1·09	0·77
La	28·9	25·3	27·8	37·0	19·8	41·1	29·1
Ce	52·9	45·6	49·8	77·2	35·2	83·4	54·0
Pr	6·64	5·75	5·86	9·58	4·69	9·98	6·62
Nd	26·4	23·8	23·4	42·8	19·9	39·9	26·8
Sm	6·00	5·28	5·31	8·93	4·62	8·31	5·80
Eu	2·19	1·82	1·87	2·85	1·66	2·87	1·93
Gd	6·03	5·50	5·09	10·9	4·77	8·67	5·77
Tb	0·91	0·71	0·76	1·00	0·75	1·15	0·80
Dy	4·83	4·13	4·45	5·62	4·33	6·19	4·54
Ho	0·83	0·72	0·74	0·90	0·81	1·04	0·81
Er	2·16	1·87	1·96	2·18	2·20	2·68	2·18
Tm	0·26	0·23	0·23	0·24	0·27	0·31	0·26
Yb	1·57	1·40	1·40	1·57	1·64	1·86	1·64
Lu	0·21	0·18	0·20	0·17	0·23	0·24	0·22

Stage:	Kāloa Volcanics						
Sample:	KV03-17	KR-2	KV03-1	PV-2	KV05-8	0301-1	KR-5	KR-11
Li	6·57	7·62	6·91	5·43	5·07	5·50	7·34	8·22
Sc	23·2	22·7	21·2	26·0	25·9	26·3	22·0	21·7
Sb	0·03	0·03	0·04	0·04	0·01	0·02	0·07	0·07
Cs	0·30	0·88	0·19	0·22	0·35	0·29	0·30	0·36
Ba	587	716	761	554	672	471	964	967
Ta	3·07	4·16	4·52	2·28	3·80	2·62	5·58	5·74
Th	3·83	6·01	5·66	2·83	3·99	3·16	7·64	6·57
U	1·14	1·25	1·02	0·86	0·97	0·71	1·79	1·97
La	31·3	47·8	52·5	27·7	38·7	33·9	69·4	54·8
Ce	62·3	94·0	102	53·1	73·8	62·4	133	117
Pr	7·79	10·5	12·7	7·01	8·53	7·25	14·7	13·9
Nd	34·6	40·3	52·5	31·8	33·2	28·9	55·0	63·2
Sm	7·28	8·18	10·6	6·83	6·87	6·10	10·5	12·4
Eu	2·42	2·77	3·42	2·25	2·24	2·08	3·54	3·79
Gd	9·55	7·32	10·5	8·96	6·31	5·66	8·99	16·3
Tb	0·86	1·07	1·33	0·91	0·92	0·87	1·27	1·27
Dy	4·80	5·55	6·47	4·97	4·69	4·46	6·12	6·79
Ho	0·85	0·81	1·05	0·88	0·74	0·73	0·90	1·10
Er	2·08	2·02	2·43	2·32	1·83	1·90	2·22	2·58
Tm	0·24	0·23	0·26	0·27	0·21	0·22	0·23	0·28
Yb	1·57	1·31	1·42	1·79	1·24	1·38	1·33	1·77
Lu	0·17	0·18	0·17	0·21	0·17	0·19	0·16	0·18

Table 3: Continued

Stage:	Post-shield						Shield			
Sample:	KV05-13	KV03-5	GA 566	GA 565	GA 650	KV05-10	KV04-21	KV04-19	KV04-16	KV04-22
Li	7·29	5·05	7·22	4·14	5·09	4·44	6·09	5·32	4·15	3·21
Sc	14·0	24·4	11·3	31·3	32·4	24·8	29·4	28·6	21·0	28·6
Sb	0·01	0·04	0·03	0·03	—	0·01	0·02	0·02	0·01	0·01
Cs	0·32	0·28	0·19	0·06	0·02	0·23	0·10	0·07	0·05	0·01
Ba	667	423	636	83·1	77·3	399	96·7	94·7	82·9	86·7
Ta	3·64	2·10	4·89	1·02	—	2·09	0·87	1·01	0·62	0·90
Th	3·94	2·31	6·88	1·01	0·76	2·61	0·79	0·94	0·73	1·00
U	0·93	0·55	1·50	0·22	0·18	0·62	0·22	0·22	0·23	0·24
La	41·6	33·0	49·7	13·9	10·7	32·5	11·5	13·4	9·7	13·6
Ce	90·0	64·6	105	32·2	26·8	59·3	28·9	32·6	24·3	32·9
Pr	10·7	7·25	14·2	4·18	4·10	7·41	3·80	4·09	3·51	3·96
Nd	44·0	29·0	61·7	17·4	19·7	29·3	17·1	17·7	17·9	16·6
Sm	10·0	6·64	14·6	4·80	5·42	6·64	4·78	4·83	4·73	4·41
Eu	3·24	2·20	5·16	1·66	1·89	2·37	1·70	1·71	1·60	1·57
Gd	8·68	6·08	14·3	4·52	5·99	6·11	4·56	4·49	5·54	4·09
Tb	1·33	0·94	2·61	0·76	0·90	0·96	0·83	0·84	0·66	0·77
Dy	6·92	5·16	15·71	5·10	5·57	5·09	4·74	4·91	4·13	4·34
Ho	1·12	0·84	3·07	0·83	1·02	0·87	0·83	0·80	0·74	0·75
Er	2·91	2·23	8·84	2·33	2·80	2·34	2·35	2·21	1·96	2·13
Tm	0·34	0·26	1·09	0·29	0·35	0·25	0·29	0·27	0·24	0·26
Yb	2·07	1·53	6·15	1·79	2·27	1·51	1·82	1·71	1·58	1·67
Lu	0·29	0·23	0·74	0·29	0·29	0·21	0·26	0·26	0·18	0·25

Trace element concentrations in ppm.

Appendix Table 3), a common feature of Hawaiian rejuvenated lavas (e.g. Clague & Frey, 1982; Yang *et al.*, 2003). There is a factor of 3·5 variation in Nb/Y, increasing with increasing Ce and correlated with rock type (foidites have higher and alkali basalts lower Nb/Y ratios; Fig. 4e), except for two samples with very low Nb/Y ($<0·5$) and high Y contents (73 and 91 ppm; Electronic Appendix Table 3). These samples have probably undergone minor secondary alteration to form a Y-rich phase (rhadophane), as suggested at another Hawaiian volcano (Kaho'olawe; Fodor *et al.*, 1992). Similar trace element ratio vs rock type correlations in the Honolulu Volcanics were attributed to a factor of five variation in degree of partial melting (Clague & Frey, 1982). An additional feature of the Kōloa Volcanics is the wide range in Nb/Y at a given Ce value (Fig. 4e), which is indicative of a heterogeneous source.

Most of the shield and post-shield samples have K_2O/P_2O_5 ratios typical of fresh Hawaiian tholeiites (1·44–1·87; e.g. Wright, 1971) confirming petrographic observations and interpretation of low LOI values that most of the shield and post-shield samples are weakly altered to

unaltered. The new XRF data for shield samples are comparable with those previously reported for the volcano, with large variations in MgO, Ni and Cr (Table 2), and a narrow and flat trend on a CaO/Al_2O_3 vs MgO plot (Fig. 4c) reflecting variable amounts of olivine fractionation and accumulation. These variations are consistent with the scarcity of cpx and plagioclase in these rocks. Some previously studied samples have lower CaO/Al_2O_3 and K_2O (Fig. 4) that may reflect alteration. Among the post-shield samples, the tholeiites are similar to the shield lavas in major elements, whereas the high-MgO alkalic post-shield samples are geochemically comparable with the Kōloa Volcanics (Fig. 4). The other alkalic post-shield samples have lower MgO (<4 wt %), Ni and Cr (<20 ppm; Table 2), typical of the hawaiitic substage of post-shield volcanism (West *et al.*, 1988).

The tholeiitic post-shield and shield samples examined here have nearly identical trace element concentrations and ratios (Figs 4 and 5; Table 2). These ratios are typical of Kea-type Hawaiian tholeiitic lavas (e.g. Zr/Nb<14; Rhodes & Vollinger, 2004). In contrast, the post-shield
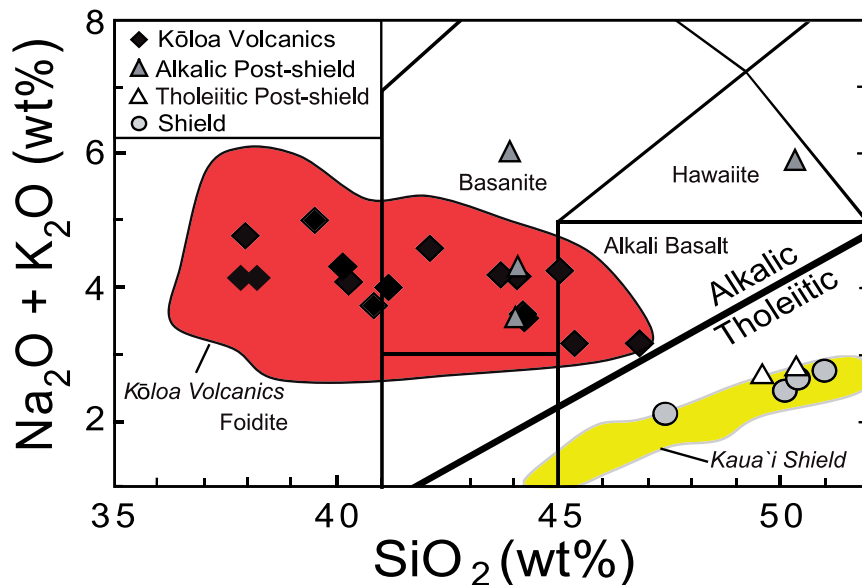
Fig. 3. Total alkalis vs silica diagram for shield, post-shield and rejuvenated (Kōloa Volcanics) lavas from Kaua'i. The samples plotted are those analyzed for isotopes. The darker gray field encloses analyses for 71 new Kōloa lavas from this study (Electronic Appendix 3). The lighter gray field is for Kaua'i shield lavas from Mukhopadhyay *et al.* (2003). The Kōloa Volcanics are exclusively alkalic, ranging in composition from alkali basalts to foidites, whereas the post-shield stage includes both tholeiitic and alkalic samples. The tholeiitic–alkalic dividing line is from Macdonald & Katsura (1964).

alkalic and Kōloa lavas have distinctly lower Zr/Nb, higher Ba/Sr values and steeper REE patterns (Figs 4 and 5). The tholeiitic shield and post-shield lavas display only moderate enrichment of highly incompatible elements, in contrast to the Kōloa and alkalic post-shield samples (Figs 4 and 5). The post-shield alkalic lavas have Nb/Y and Zr/Nb ratios overlapping the weakly alkalic Kōloa lavas, consistent with their major element chemistry (Figs 3 and 4e). A hawaiite sample is distinct on elemental plots (Figs 4 and 5). All of the new Kaua'i rocks have similar heavy REE (HREE) values despite the wide range in light REE (LREE; Fig. 5; note the linear rather than usual log scale, allowing more details to be seen). The nearly constant HREE abundances and crossing REE patterns indicate the presence of garnet in the source of these lavas (similar features are seen for other Hawaiian alkalic lavas; e.g. Lōihi, Garcia *et al.*, 1995; Kohala, Lanphere & Frey, 1987). The wide range in incompatible trace element ratios of Kaua'i lavas is indicative of multiple sources (Ba/Sr and Zr/Nb; e.g. Frey *et al.*, 2005) and variable degrees of partial melting (Nb/Y; e.g. Clague & Frey, 1982).

ISOTOPIC COMPOSITIONS OF KŌLOA, KAUA'I SHIELD AND POST-SHIELD LAVAS

The new high-precision isotopic data for the Kōloa Volcanics (Table 4) extend the known ranges for Pb, Sr,

Nd and Hf ratios for this rock group. The Kōloa Pb data form a well-defined linear array (correlation coefficient R^2 of 0·99) in $^{208}Pb/^{204}Pb$ vs $^{206}Pb/^{204}Pb$ space, with two samples from the same lava flow (KR-5 in duplicate and KR-11) having the highest $^{206}Pb/^{204}Pb$ ratios reported for rejuvenated lavas, and among the highest reported for any Hawaiian lava (Fig. 6a). Ignoring these two samples, the Pb ratios of the Kōloa Volcanics overlap with those of Kaua'i shield and post-shield samples. However, the tholeiitic post-shield and new shield samples have higher $^{208}Pb/^{204}Pb$ ratios for a given $^{206}Pb/^{204}Pb$ ratio, whereas the alkalic post-shield samples have slightly lower $^{208}Pb/^{204}Pb$ ratios for a given $^{206}Pb/^{204}Pb$ ratio, as do previous shield samples (Fig. 6a).

The Hf isotopic data (Table 4) are the first for Kaua'i's shield and post-shield stages, and supplement six previous values for Kōloa Volcanics (Stracke *et al.*, 1999). The ε_{Hf} vs $^{206}Pb/^{204}Pb$ plot (Fig. 6b) displays a clear distinction between tholeiitic (positive trend) and alkalic samples (negative trend). The Kaua'i tholeiites plot along the hyperbola for Hawaiian shield lavas, whereas the alkalic lavas and other Hawaiian rejuvenated lavas plot above this hyperbola (except for the one high $^{206}Pb/^{204}Pb$ sample; Fig. 6b). A similar pattern is exhibited on an ε_{Nd} vs $^{206}Pb/^{204}Pb$ plot (Fig. 6c). The Kōloa lavas have low Sr isotopic ratios (0·70296–0·70325), the lowest for any suite of Hawaiian rejuvenated lavas (Fig. 6d and e). Kaua'i shield stage lavas have higher Sr values (0·70345–0·70381) similar to other
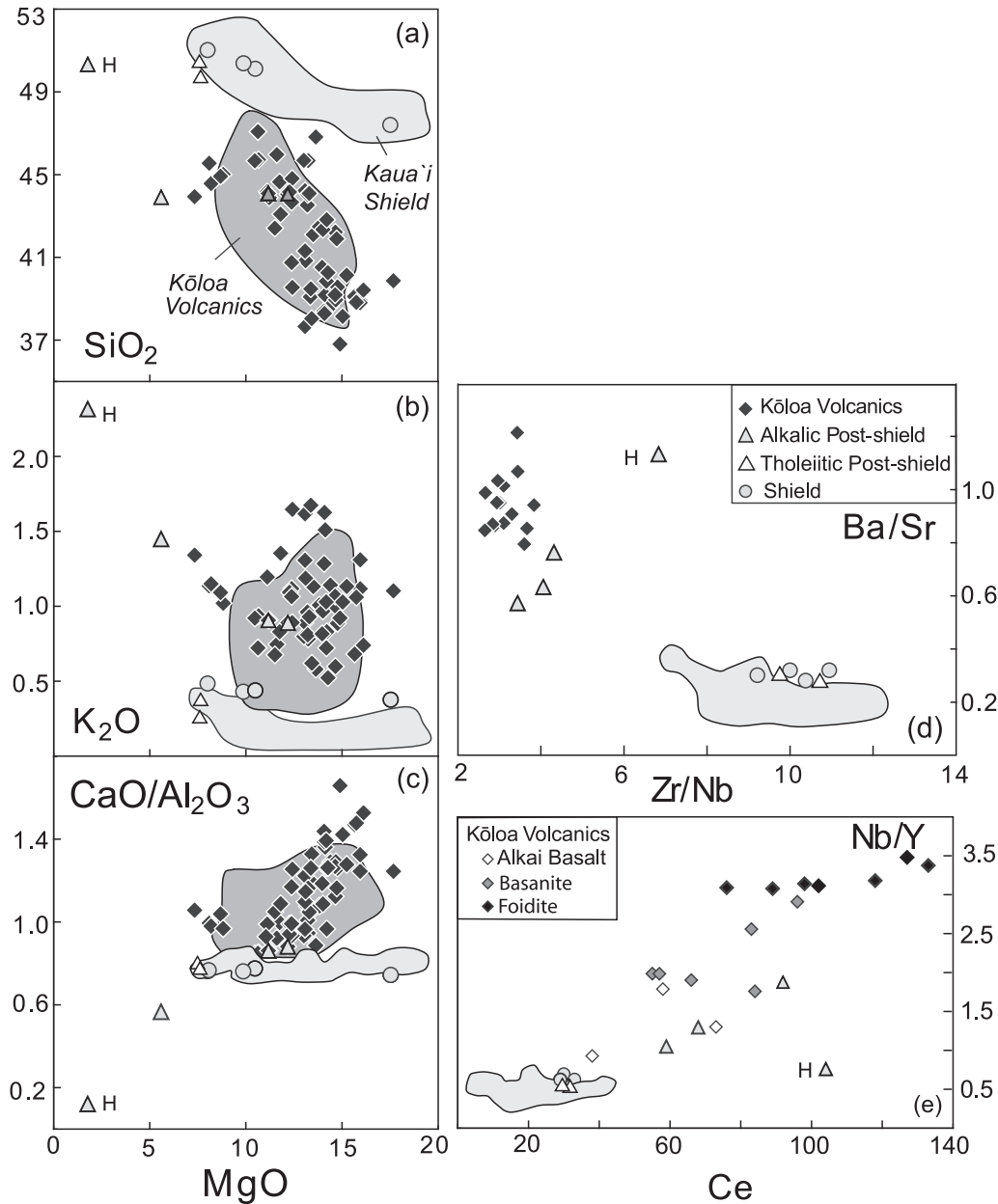
Fig. 4. XRF major and trace element abundance and ratio plots comparing the shield, post-shield and rejuvenated stages of Kaua'i volcanism. (a) SiO_2 vs MgO; (b) K_2O vs MgO; (c) CaO/Al_2O_3 vs MgO; (d) Ba/Sr vs Zr/Nb. The shield and rejuvenated stages define two distinct groups in this plot. The post-shield lavas also form two groups: the tholeiitic samples plot near the shield stage lavas whereas the alkalic samples plot near the rejuvenated stage lavas. (e) Nb/Y vs Ce. Rock type (as defined in Fig. 3) correlates with Nb/Y, indicating that foidites result from lower degrees of partial melting and alkalic basalts result from higher degrees of partial melting. Kaua'i shield represented by light gray field (from Mukhopadhyay *et al.*, 2003). Kōloa Volcanics from previous studies in darker gray field (Clague & Dalrymple, 1988; Maaløe *et al.*, 1992; Reiners & Nelson, 1998). The 'H' on the plots represents the geochemically distinct hawaiite sample, GA 566.

Hawaiian shields (Fig. 6). There is also a Sr isotopic distinction between alkalic and tholeiitic post-shield samples; the tholeiites plot within the Kaua'i shield field, whereas the alkalic samples plot with Kōloa lavas (Fig. 6d and e). The new Kaua'i shield isotope results overlap those from

previous studies but extend to higher $^{208}Pb/^{204}Pb$ at a given $^{206}Pb/^{204}Pb$ and fall within the Loa field (Fig. 6). These isotopic differences may reflect the observed regional trends in isotope values (Reiners *et al.*, 1999; Mukhopadhyay *et al.*, 2003). Our samples are from a

Fig. 5. Rare earth element (REE) diagram (ICP-MS data) for Kaua'i volcanic rocks. REE values normalized to chondrite values from McDonough & Sun (1995). The wide range in LREE abundances but nearly constant HREE abundances and the crossing REE patterns should be noted. Both features are indicative of garnet in the source for these lavas. Scale is linear to better show small-scale features. The 2σ error bars are within the size of the symbol.

previously unanalyzed area on the SE flank of Kaua'i shield (Fig. 1) and fall at the higher end of these trends, consistent with their geographical location.

A temporal variation is observed in some isotopic ratios for the 4·5 Myr of Kaua'i volcanism (Fig. 7). There is an overall trend towards higher $^{143}Nd/^{144}Nd$ and ε_{Hf}, and lower $^{87}Sr/^{86}Sr$ with decreasing age. In detail, the isotopic differences are related to rock type; the alkalic post-shield and rejuvenated lavas are similar, and distinct from the tholeiites (Fig. 7). In contrast, $^{206}Pb/^{204}Pb$ values range widely and overlap for shield, post-shield and rejuvenated lavas. Among the Kōloa samples, the ranges for Pb, Sr and Nd isotopes narrow at <1·5 Ma with flat trends for $^{87}Sr/^{86}Sr$ and $^{143}Nd/^{144}Nd$ ratios, and a decreasing trend in $^{206}Pb/^{204}Pb$. In contrast, no temporal isotopic pattern is evident for Honolulu Volcanics (Fekiacova *et al.*, 2007).

REJUVENATED VOLCANISM
Source lithology and parental magma composition

It is commonly recognized that oceanic island rejuvenated alkalic lavas are produced by low-degree partial melting of the mantle source (e.g. Clague & Frey, 1982; Yang *et al.*, 2003; Geldmacher *et al.*, 2005), although there is considerable controversy about the conditions of magma generation. Here we evaluate the primary magma compositions, source lithology and the melting conditions that produce rejuvenated lavas to better understand the origin of these lavas. Primary magma compositions, mantle

potential temperatures and source melt fractions for the Kōloa Volcanics were calculated from primitive (high-MgO) whole-rock compositions using PRIMELT2.XLS software (Herzberg & Asimow, 2008). Details of the computational method have been given by Herzberg & O'Hara (2002), Herzberg *et al.* (2007) and Herzberg & Asimow (2008). Briefly, the program calculates a primary magma composition by incremental addition of olivine to bring a lava composition into equilibrium with a fertile peridotite composition (KR-4003; Walter, 1998). The isotopic results, however, show that the source for Kōloa lavas was depleted but no experimental data are available for appropriate compositions. All calculated primary magma compositions are assumed to be derived by accumulated fractional melting of this fertile peridotite. Uncertainties in fertile peridotite composition affect the estimated melt fraction but have less impact on mantle potential temperature values (Herzberg & O'Hara, 2002; Herzberg & Asimow, 2008). PRIMELT2.XLS calculates the olivine liquidus temperature at 1 atm (±31°C at the 2σ level of confidence; Herzberg & Gazel, 2009). The mantle potential temperature estimates have a precision that is similar to the accuracy of the olivine liquidus temperature. The temperature and melt fraction estimates are dependent on model input parameters, which assume no clinopyroxene fractionation in the mantle. Accumulated fractional melts are produced by the mixing of instantaneous fractional melts that are generated by decompression from an initial to a final melting pressure (Herzberg & Asimow, 2008). All melt

Table 4: Pb, Sr, Nd and Hf isotope data for Kōloa, post-shield and shield stage lavas from Kauaʻi

Sample	$^{206}Pb/^{204}Pb$	±	$^{207}Pb/^{204}Pb$	±	$^{208}Pb/^{204}Pb$	±	$^{87}Sr/^{86}Sr$	±	$^{143}Nd/^{144}Nd$	±	ε_{Nd}	$^{178}Hf/^{177}Hf$	±	ε_{Hf}
Kāloa Volcanics														
KV03-11	18·1361	21	15·4474	20	37·7857	54	0·703201	7	0·513066	6	8·25	—	—	—
KV03-11 dup	18·1402	9	15·4517	13	37·7957	47	0·703209	6	0·513065	7	8·23	—	—	—
KV05-2	18·0895	11	15·4316	10	37·7794	27	0·703165	5	0·513048	5	8·00	—	—	—
KV05-1	18·1373	7	15·4356	6	37·7840	17	0·703165	8	0·513049	8	8·02	—	—	—
KV03-15	18·1754	23	15·4552	21	37·8472	51	0·703156	7	0·513044	7	7·92	0·283149	11	13·34
KV04-1	18·2130	6	15·4509	5	37·8613	15	0·703162	6	0·513055	6	8·13	—	—	—
KV03-21	18·2423	14	15·4546	13	37·9105	36	0·703176	7	0·513048	7	8·00	—	—	—
KV04-4	18·1402	15	15·4426	14	37·7670	40	0·703070	6	0·513087	6	8·76	—	—	—
KV03-17	18·1404	8	15·4386	7	37·7642	19	0·703008	6	0·513072	6	8·47	0·283165	6	13·90
KR-2	18·2239	7	15·4486	7	37·8731	21	0·703055	6	0·513059	6	8·21	—	—	—
KV03-1	18·3206	16	15·4603	15	38·0253	33	0·703130	7	0·513016	7	7·37	—	—	—
PV-2	18·2932	7	15·4539	6	37·9961	16	0·703243	5	0·513025	5	7·55	—	—	—
KV05-8	18·1984	8	15·4483	9	37·8518	23	0·702959	8	0·513077	8	8·56	—	—	—
0301-1	18·2023	8	15·4405	7	37·9104	19	0·703248	6	0·513019	6	7·43	—	—	—
KR-11	18·5714	49	15·4848	45	38·3315	109	0·703113	7	0·513012	7	7·29	—	—	—
KR-5	18·6136	17	15·4771	15	38·3757	44	0·703092	8	0·513022	6	7·48	0·283083	7	10·99
KR-5 (2)M	18·6044	17	15·4777	18	38·3575	42	—	—	—					
Post-shield														
KV05-13*	18·1989	8	15·4537	6	37·8285	16	0·703221	6	0·513054	6	8·11	—	—	—
KV03-5*	18·1198	19	15·4432	13	37·7380	30	0·703168	8	0·513064	6	8·31	0·283189	5	14·76
GA 566M*	18·3290	6	15·4697	5	37·9403	14	0·703421	7	0·513034	9	7·72	0·283134	6	12·81
GA 565M	18·1848	5	15·4512	5	37·9735	13	0·703721	8	0·512937	3	5·82	0·283072	5	10·61
GA 650M	18·1794	7	15·4481	7	37·9005	18	0·703697	7	0·512963	7	6·35	0·283087	4	11·15
GA 650 rep	18·1791	8	15·4488	8	37·9017	16	—	—	—	—	—	—	—	—
KV05-10*	18·1859	7	15·4568	5	37·7986	17	0·703183	8	0·513069	6	8·40	0·283177	5	14·33
Shield														
KV04-21	18·1116	4	15·4478	4	37·8834	11	0·703771	9	0·512944	8	5·96	0·283072	6	10·60
KV04-19	18·2133	6	15·4555	6	37·9697	16	0·703745	7	0·512970	8	6·47	0·283088	11	11·17
KV04-16	18·1857	7	15·4540	8	37·9563	19	0·703758	7	0·512946	7	6·00	0·283069	6	10·50
KV04-16 dupM	18·1855	5	15·4542	4	37·9565	14	0·703745	7	0·512952	7	6·12	0·283077	7	10·80
KV04-22	18·0861	10	15·4453	8	37·9250	22	0·703830	10	0·512897	7	5·05	0·283063	6	10·30
KV04-22 rep	18·0855	5	15·4446	5	37·9244	13	—	—	—	—	—	—	—	—
BHVO-2 ref.	18·6451	6	15·4878	4	38·2018	23	0·703460	10	0·513005	7	7·16	0·283099	4	11·57

*Alkalic post-shield samples; remaining post-shield samples are tholeiitic.
Koloa Volcanics are listed in increasing age order. rep, same solution ran twice; dup, completely new dissolution of same sample; errors (±) are 2σ with only the last digits shown. All samples were leached using method outlined by Weis & Frey (1991, 1996), Weis *et al.* (2005) and Nobre Silva *et al.* (2009). Samples were analyzed for Pb and Hf by MC-ICP-MS using a Nu Plasma Instruments system; for Sr by TIMS using a Finnigan TRITON system. Samples denoted with M were analyzed for Nd by MC-ICP-MS; remaining samples analyzed for Nd by TIMS using a TRITON system. USGS reference BHVO-2 was run twice for Pb isotopes; average reported with difference indicated as error (for characterization of this sample, see Weis *et al.*, 2006).

fractions calculated with PRIMELT2 are strictly valid for fertile peridotite. However, different peridotite compositions will produce primary magmas with similar MgO at similar conditions of melting, although less liquid volume is obtained from depleted peridotite (Herzberg & O'Hara, 2002).

The low SiO_2 and high CaO of most Kōloa lavas lie outside the calibration of PRIMELT2 (Fig. 8). Similar lava compositions are found on many oceanic islands and are thought to have formed as low-degree melts of carbonated peridotite (Dasgupta *et al.*, 2007). However, four of the higher SiO_2 Kōloa lavas (45–46 wt %) yielded
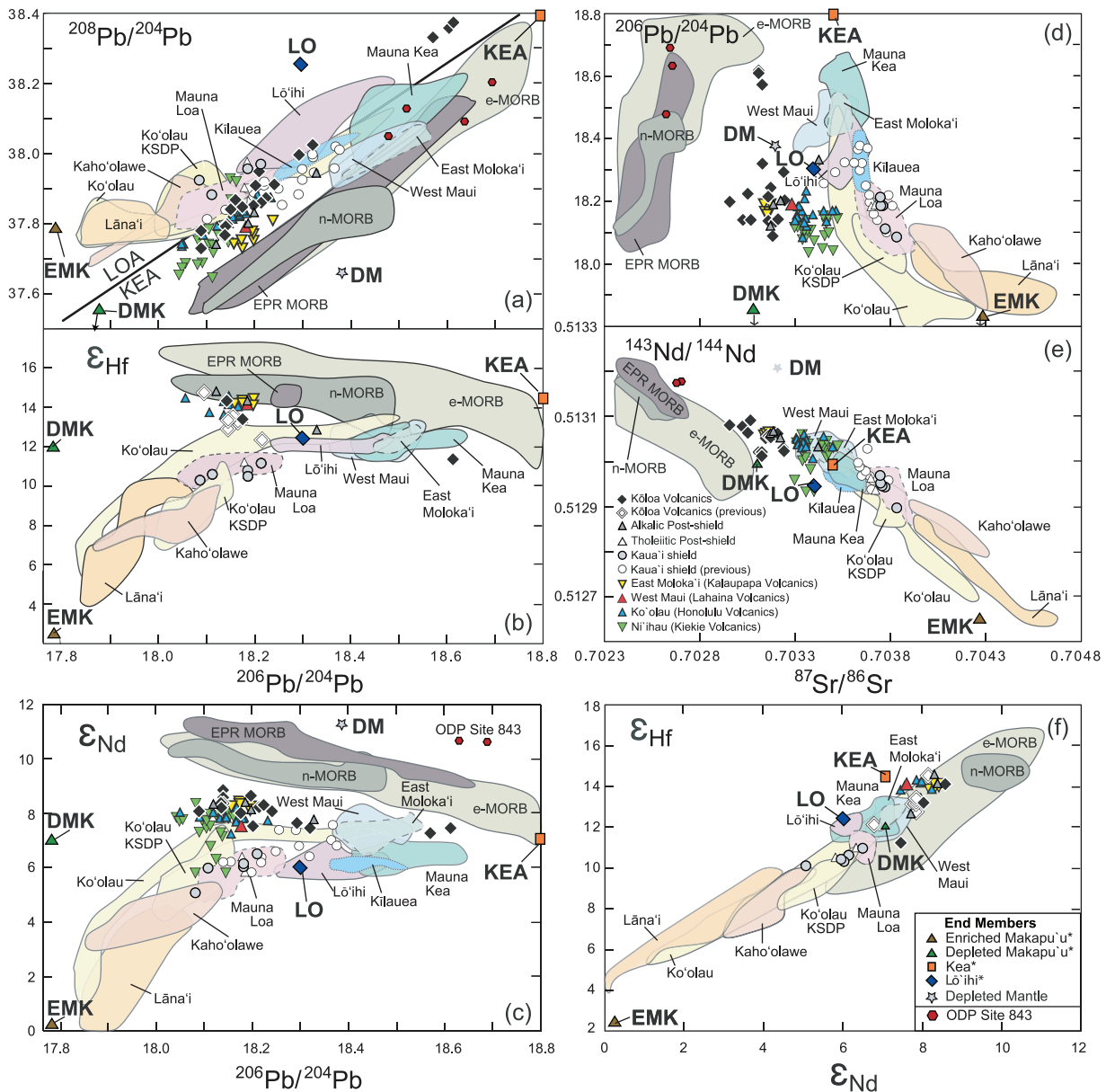
Fig. 6. Comparison of Pb, Hf, Sr and Nd isotopic compositions of the different stages of Kaua'i volcanism with rejuvenated and shield volcanism from other Hawaiian Islands. (a) $^{208}Pb/^{204}Pb$ vs $^{206}Pb/^{204}Pb$. The line on the graph is the Loa–Kea boundary from Abouchami *et al.* (2005). (b) ε_{Hf} vs $^{206}Pb/^{204}Pb$. The tholeiitic shield Kaua'i lavas plot along and near the middle of the mixing hyperbola defined by the other Hawaiian shield volcanoes (Blichert-Toft *et al.*, 1999), whereas the alkalic Kaua'i lavas, Kōloa Volcanics and all other Hawaiian rejuvenated lavas trend away from this hyperbola to higher ε_{Hf} values. This pattern indicates that at least three end-member components were sampled by these lavas. (c) ε_{Nd} vs $^{206}Pb/^{204}Pb$. (d) $^{206}Pb/^{204}Pb$ vs $^{87}Sr/^{86}Sr$. Most Kaua'i shield lavas plot on the mixing hyperbola with the other Hawaiian shield lavas, with the exception of some Kaua'i lavas inferred to have sampled depleted mantle (Mukhopadhyay *et al.*, 2003). The rejuvenated lavas (Kōloa, Honolulu, Kalaupapa and Lahaina) all trend towards a depleted component different from the East Pacific Rise MORB. (e) $^{143}Nd/^{144}Nd$ vs $^{87}Sr/^{86}Sr$. (f) ε_{Hf} vs ε_{Nd}. Sources of isotopic data (Pb, Sr, Nd, Hf) are: Kīlauea, Chen *et al.* (1996), Blichert-Toft *et al.* (1999) and Abouchami *et al.* (2005); Mauna Kea, Abouchami *et al.* (2000) and Blichert-Toft *et al.* (2003); Mauna Loa, Abouchami *et al.* (2000), Blichert-Toft *et al.* (2003), Tanaka & Nakamura (2005), Wanless *et al.* (2006) and Marske *et al.* (2007); Lāna'i, Gaffney *et al.* (2005); Ko'olau, Stille *et al.* (1983), Roden *et al.* (1994), Abouchami *et al.* (2005) and Fekiacova *et al.* (2007); Kaho'olawe, Leeman *et al.* (1994) and Huang *et al.* (2005); Lōihi, Staudigel *et al.* (1984), Blichert-Toft *et al.* (1999) and Abouchami *et al.* (2005); Haleakalā, West *et al.* (1987), Chen *et al.* (1991) and Blichert-Toft *et al.* (1999); West Maui, Gaffney *et al.* (2004); East Moloka'i, Xu *et al.* (2005); West Moloka'i, Stille *et al.* (1986) and Xu *et al.* (2007); ODP Site 843, Fekiacova *et al.* (2007); EPR and E-MORB, Niu *et al.* (1999) and Castillo *et al.* (2000); N-MORB, Mahoney *et al.* (1992, 1994), Salters (1996), Nowell *et al.* (1998), Salters & White (1998), Chauvel & Blichert-Toft (2001), Kempton *et al.* (2002) and Janney *et al.* (2005). End-members for Hawaiian lavas [Kea, Lo (Lōihi), DM (depleted ancient mantle), DMK (depleted Makapuu Ko'olau) and EMK (enriched Makapuu Koolau)] from Tanaka *et al.* (2002, 2008). The 2σ error bars are within the size of the symbol.

Fig. 7. Temporal variation in Pb, Sr, Nd and Hf isotopic ratios for the rejuvenated, post-shield and shield stages of Kaua'i volcanism. The vertical bar with stippled pattern represents the previous spread in isotopic ratios for Kaua'i shield lavas (from Mukhopadhyay *et al.*, 2003); no age data available for these samples. Vertical gray bar in (d) is for previous analyzed but undated Kōloa Volcanics (Stracke *et al.*, 1999). During the rejuvenated stage, the isotopic heterogeneity decreased abruptly at 1·5 Ma. No simple correlation is seen between age and rock type for Kaua'i volcanism, although the shield samples exhibit higher Sr and lower Nd isotope ratios relative to Kōloa lavas and the Kōloa lavas show a general decrease in Pb isotope ratios. The post-shield samples exhibit a relatively large isotopic range over a small time scale. The 2σ error bars for the isotopic ratios and ages are within the size of the symbol.

successful solutions after addition of 12–21% olivine (Table 5). The PRIMELT2 results indicate that the primary magmas of Kōloa Volcanics contained 17–18 wt % MgO, ~10 wt % CaO and 10–11 wt % FeO (Fig. 9; Table 5). The degree of partial melting for the Kōloa samples was estimated to be 0·02–2·6%. Calculated mantle temperatures for these Kōloa lavas are remarkably consistent and high (1515–1534°C; Table 5) indicating melting from anomalously hot mantle (100–200°C above ambient mantle). These estimates of low degrees of partial melting and high mantle potential temperatures for the Kōloa rejuvenated lavas are similar to estimates for other Hawaiian volcanoes (<2% melting; e.g. Yang *et al.*, 2003; ~1450–1550°C; Putirka *et al.*, 2005, 2007; Herzberg *et al.*, 2007) and other oceanic islands (e.g. Cape Verde Islands; Holm *et al.*, 2006). PRIMELT2 modeling results also indicate moderate melting pressures (3·5–4 GPa; Fig. 9). These results are consistent with the flexural arch model for rejuvenated volcanism (Bianco *et al.*, 2005), which has melting occurring in the upper part of the plume. These moderate pressures are not compatible with the secondary zone model of Ribe & Christensen (1999), which has melting at the base of the plume. Although the calculated mantle potential temperatures are high, the melt fractions are low because the thick lithosphere did not permit a significant amount of melting.

Source lithology is also constrained by PRIMELT2 modeling because melts of spinel peridotite, garnet peridotite and pyroxenite in olivine–anorthite–diopside–silica projection space do not overlap (Herzberg *et al.*, 2008). The four calculated primary magmas for the Kōloa lavas (Fig. 9, Table 5) all indicate a garnet peridotite $(Ol + Opx + Cpx + Gt)$ source mineralogy, consistent with evidence from REE and other geochemical data (Fig. 5). Results for primary magma compositions from depleted garnet peridotite have similar major-element compositions to those of fertile garnet peridotite at similar melting conditions, although at lower degrees of melting and producing less than half the amount of melt (Herzberg & O'Hara, 2002; Herzberg & Asimow, 2008). As discussed below, existing causative models for rejuvenated volcanism are unable to produce the volume or the flux rate of magma observed for the Kōloa Volcanics. Thus, a strongly depleted source [i.e. normal mid-ocean ridge basalt (N-MORB)-source mantle] is unlikely to produce the observed volume of rejuvenated lavas on Kaua'i. PRIMELT2 did not provide successful solutions from a garnet pyroxenite source for the Kōloa primary magma composition (e.g. CaO was significantly lower than in the Kōloa Volcanics; Fig. 9).

In summary, the PRIMELT2 modeling provides evidence for the Kōloa lavas being derived from high-MgO (17–18 wt %) primary magmas formed by low degrees of partial melting (0·02–2·6%) at moderate
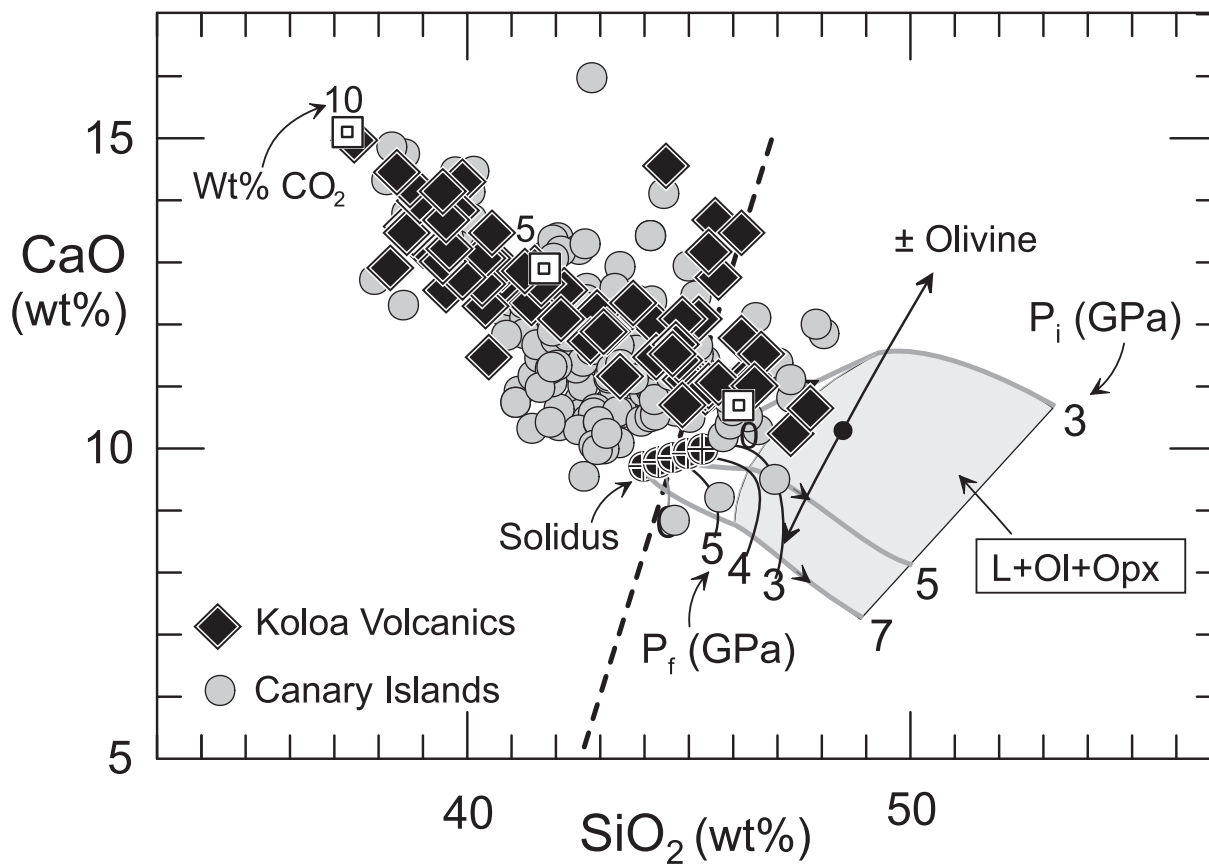
Fig. 8. SiO_2 and CaO abundances in the Kōloa Volcanics compared with partial melts of carbonated peridotite (from Dasgupta *et al.*, 2007), lavas from the Canary Islands, and estimated primary melts of fertile peridotite from Herzberg & Asimow (2008). Curves for liquids derived from accumulated fractional melting of anhydrous, fertile peridotite are from Herzberg & Asimow (2008). The thick gray curved lines are for initial melting; black curves are for final melting. The dashed, thick black line divides CO_2-enriched and CO_2-depleted lavas, which is a filter used by Herzberg & Asimow (2008) for high-CaO, low-SiO_2 lavas that may have formed from carbonated peridotite. The peridotite partial melting experiments of Dasgupta *et al.* (2007) with 0, 5 and 10 wt % CO_2 at 3 GPa are shown as four black and white boxes. Lava compositions from the Canary Islands with MgO >10 wt % and higher CaO (above the black discriminant line in MgO–CaO in Fig. 9b) are from the GEOROC database (http://georoc.mpch-mainz.gwdg.de/georoc/). The Kōloa lavas follow the trend of the CO_2 array defined by the experiments of Dasgupta *et al.* (2007), overlapping with the Canary Islands high-CaO, low-SiO_2 lavas. The four successful PRIMELT2 models for Kōloa lavas, shown in Fig. 9a, lie on the high-SiO_2 side of the dashed black line.

pressures (3·5–4·0 PGa) from a garnet peridotite source with high mantle potential temperatures ($1525 \pm 10°C$). Thus, a plume source is the most likely origin for Kōloa magmas. This hypothesis is evaluated with isotopic evidence below.

NATURE AND DISTRIBUTION OF MANTLE SOURCES FOR KŌLOA VOLCANICS

The source of Hawaiian rejuvenated volcanism has long been debated (e.g. Jackson & Wright, 1970; Clague & Frey, 1982; Gurriet, 1987; Lassiter *et al.*, 2000; Yang *et al.*, 2003; Frey *et al.*, 2005; Dixon *et al.*, 2008). The duration of the debate reflects the problematic geochemical nature of

these lavas: isotopic data indicate a depleted source but trace element compositions suggest an enriched one (Figs 4–6). These contrasting features have been attributed to (1) very small degree melting of depleted mantle (N-MORB source), (2) larger degree melting of recently enriched source (plume), and (3) mixing of melts from enriched and depleted sources (e.g. Reiners & Nelson, 1998; Yang *et al.*, 2003).

An N-MORB source is unlikely based on the trace element and isotope data (Figs 6 and 10). For example, on a plot of Nb/Y vs Zr/Y, the rejuvenated lavas form a coherent trend distinct from the MORB trend (Fig. 10). Extremely low degrees of melting ($<0·1\%$) would be required to create the elevated Nb/Y values of the Kōloa lavas (Fig. 10), which is both problematic to erupt and to produce the large observed volume of Kōloa lavas ($\sim58 \text{ km}^3$).

Table 5: Estimated primary magma compositions and melting conditions for Kōloa Volcanics

Sample:	PV-1	PV-2	0622-6	KV03-20	Average
SiO_2	44·59	45·01	45·62	45·62	45·42
TiO_2	2·00	1·66	1·64	1·79	1·70
Al_2O_3	9·87	10·27	10·60	10·50	10·45
Cr_2O_3	0·08	0·06	0·06	0·08	0·07
Fe_2O_3	0·99	0·82	0·82	0·89	0·84
FeO	11·20	11·09	10·64	10·53	10·75
MnO	0·20	0·20	0·18	0·19	0·19
MgO	18·18	18·20	17·34	17·36	17·63
CaO	9·25	9·57	9·79	9·88	9·75
Na_2O	2·45	2·02	2·30	2·07	2·13
K_2O	0·77	0·58	0·64	0·71	0·64
NiO	0·10	0·11	0·11	0·09	0·10
P_2O_5	0·33	0·41	0·27	0·31	0·33
Eruption T (°C)	1413	1413	1396	1396	1402
Potential T (°C)	1534	1534	1515	1516	1522
Melt fraction	0·002	0·012	0·006	0·026	0·01
% Olivine added	17·0	21·3	16·8	12·3	16·8

Total iron adjusted to 92% FeO. Compositions normalized to 100% total (see text for methods).

A mantle source enriched in trace elements will more easily produce compositions similar to the Kōloa lavas at higher degrees of partial melting. Yang *et al.* (2003) suggested addition of low-degree melts from enriched mantle into a depleted source to explain the rejuvenated Honolulu Volcanics, although the identity of this source cannot be evaluated from trace element data alone.

High-resolution Pb isotope data also help constrain the Kōloa source. For example, the involvement of the Pacific lithosphere in the generation of the rejuvenated lavas can be evaluated using (1) the ~110 Ma lithosphere near Hawai'i, sampled from ODP Site 843 located 300 km west of the island of Hawai'i (Fig. 1) and (2) present-day basalts from the East Pacific Rise (EPR). The Kōloa Hf and Pb isotope data trend toward a depleted mantle component with lower $^{206}Pb/^{204}Pb$ ratios than those of EPR MORB or ODP Site 843 basalts, and with significantly more radiogenic $^{207}Pb/^{204}Pb$ and $^{208}Pb/^{204}Pb$ (Fig. 6a). Also, the Kōloa Volcanics define a Pb–Pb isotope trend line that does not intersect the ODP Site 843 lavas or the EPR MORB field as was also noted for the Honolulu Volcanics (Fekiacova *et al.*, 2007). Comparison of the Kōloa isotopic data with those from the literature for Hawaiian xenoliths does not indicate a direct relationship

with a Pacific lithosphere source. For example, the MORB-related Hualālai gabbro xenoliths have similar Pb isotope ratios but show no overlap in either $^{87}Sr/^{86}Sr$ (all lower than 0·7028) or $^{143}Nd/^{144}Nd$ (ϵ_{Nd} all higher than 8·4) with the Kōloa rejuvenated lavas (Lassiter & Hauri, 1998). Thus, the Pacific lithosphere is not likely to be a source for the Kōloa lavas. If the depleted component is part of the Hawaiian plume, how and where is it distributed?

Kōloa lavas lie off the well-defined Hawaiian shield Hf–Pb and Nd–Pb arcuate arrays plotting above and near the middle of the array near the Kaua'i shield lavas (Figs 6b and c), suggesting that these lavas were derived by variable mixtures of at least three source components. Surprisingly, most Hawaiian rejuvenated lavas also project away from the middle region of the Hf–Pb and Nd–Pb arrays (Fig. 6) rather than near the composition of the underlying shield (e.g. East Moloka'i and Ko'olau; Fig. 6). Thus, the sources for all Hawaiian rejuvenated lavas are remarkably similar. However, each group of rejuvenated lavas forms separate linear trends in high-precision Pb–Pb isotope space (Fig. 11b), indicating local heterogeneity in the source and that much of the variation is dominated by two components with possible involvement of a third component.

Potential explanations for the presence of the depleted component mainly during the rejuvenated and post-shield stages of Hawaiian volcanism are: (1) it is volumetrically minor within the Hawaiian plume and is swamped by melts from more refractory components during the shield stage; and/or (2) it is concentrated on the margins of the plume and sampled mainly during the later stages of volcanism (e.g. Fekiacova *et al.*, 2007). However, the recognition of the depleted component in shield lavas from the northern Emperor Seamounts, Kaua'i and Ko'olau volcanoes indicates that the depleted mantle (DM) component is not confined to its margins and is a long-lived part of the Hawaiian plume (Mukhopadhyay *et al.*, 2003; Frey *et al.*, 2005; Salters *et al.*, 2006). It should be noted that each of these studies has defined the DM component somewhat differently. Thus, the extent of melting and relative volume of the source components are probably the key factors in controlling the presence of the depleted component in Hawaiian lavas (Fig. 6).

The Kōloa samples with extremely high $^{206}Pb/^{204}Pb$ ratios (Fig. 6a) indicate involvement of an additional, previously unknown source component, characterized by high $^{206}Pb/^{204}Pb$ and $^{208}Pb/^{204}Pb$ ratios and lower ϵ_{Hf} (Fig. 6). These samples are from one of the oldest and most silica-undersaturated Kōloa lava (melilite nephelinite; Table 2). Thus, this component may be sampled only by very low degrees of melting during the early part of the rejuvenated stage.
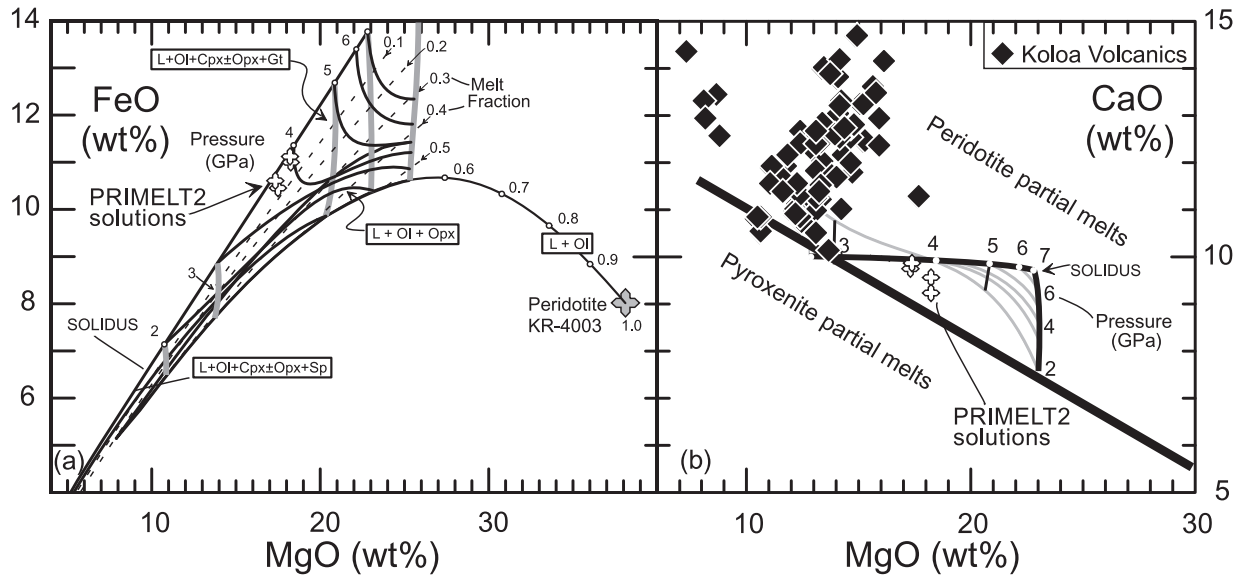
Fig. 9. Estimated primary magma compositions for four Kōloa Volcanic samples (samples KV03-20, PV-2, 0622-6, PV-1) using the modeling technique of Herzberg & Asimow (2008). Kōloa compositions and modeling results are overlain on diagrams provided by C. Herzberg. (a) FeO vs MgO for Kōloa lava compositions and results from forward model for accumulated fractional melting of fertile garnet peridotite KR-4003 (Kettle River Peridotite, molar Mg-number of 89·4; Walter, 1998). Mole fraction Fe^{2+}/total Fe is 0·90. White crosses show results from olivine addition (inverse model) using PRIMELT2 (Herzberg & Asimow, 2008). (b) CaO vs MgO with PRIMELT2 modeling results (white crosses) for Kōloa Volcanics. Potential parental magma compositions with >45 wt % SiO_2 and higher MgO and CaO contents were selected. Olivine was incrementally added to the selected compositions using PRIMELT2 software to show an array of potential primary magma compositions (inverse model). The results from the inverse model are compared with a range of accumulated fractional melts from anhydrous fertile peridotite, derived by parameterization of experimental results using the forward model of Herzberg & O'Hara (2002). A melt fraction was sought that was unique to both the inverse and forward models (Herzberg et al., 2007; Herzberg & Asimow, 2008). A unique solution was found when there was a common melt fraction for both models in FeO–MgO and CaO–MgO–Al_2O_3–SiO_2 (CMAS) projection space. This modeling assumes that olivine was the only phase crystallizing and ignores chromite precipitation, and possible augite fractionation in the mantle (Herzberg & O'Hara, 2002). Results from PRIMELT2 indicate a residue of garnet peridotite (not spinel peridotite or harzburgite/dunite/pyroxenite). Curve for initial melting pressure at 4 GPa not shown in (a) for clarity. Dashed curves in (a) indicate melt fraction. Solidi for spinel and garnet peridotite are labeled in (a). Thick black line in (b) divides potential melts from peridotite vs pyroxenite based on the results from Herzberg (2006).

A carbonatite or carbonated peridotite source component for Kōloa lavas?

CO_2 has been suggested to play an important role in generating rejuvenated lavas on Kaua'i, Ni'ihau (e.g. Maaløe et al., 1992; Dixon et al., 2008) and other ocean islands (e.g. Cape Verde Islands, Silva et al., 1981; Canary Islands, Hoernle et al., 2002). The low degree of partial melting needed to generate these strongly alkalic lavas enhances the potential effects of CO_2 (e.g. Dasgupta et al., 2007). Experiments on garnet peridotite with 0·1–0·25 wt % CO_2 produce ocean island-like carbonated silicate melts from 1–5% melting (e.g. Dasgupta et al., 2007). These melts are enriched in CaO and depleted in SiO_2, similar to the rejuvenated lavas from Kaua'i and the Canary Islands (Fig. 8). Is the CO_2 coming from carbonate in the source? A trend of decreasing Nb/La with increasing Ba/Th is inferred to be a signature for melting a carbonated peridotite or a carbonatite source (Dixon et al., 2008). High Ba/Th reflects the high Ba and low Th contents of carbonatites (e.g. Hoernle et al., 2002; Dixon et al., 2008).

Ba/Th ratios of Kōloa lavas are relatively low (<200) and completely overlap the values of Kaua'i shield tholeiites, in contrast to those of the Ni'ihau rejuvenated lavas (200–355; Dixon et al., 2008). A tiny carbonatite component (up to 0·2 vol. %) has been invoked to explain the high Ba/Nb in the Ni'ihau lavas (Dixon et al., 2008). Thus if there is any carbonatite contribution to the source for the Kōloa lavas, it was extremely minor (<0·1 vol. %). Low Ba/Th and high Nb/La in North Arch lavas and Honolulu Volcanics were used to infer that these lavas also did not have a carbonatite contribution (Yang et al., 2003). An alternative explanation for the low SiO_2 and high CaO in the Kōloa rocks is the high CO_2 content in the source (Dasgupta et al., 2007).

KAUA'I SHIELD AND POST-SHIELD MANTLE SOURCES

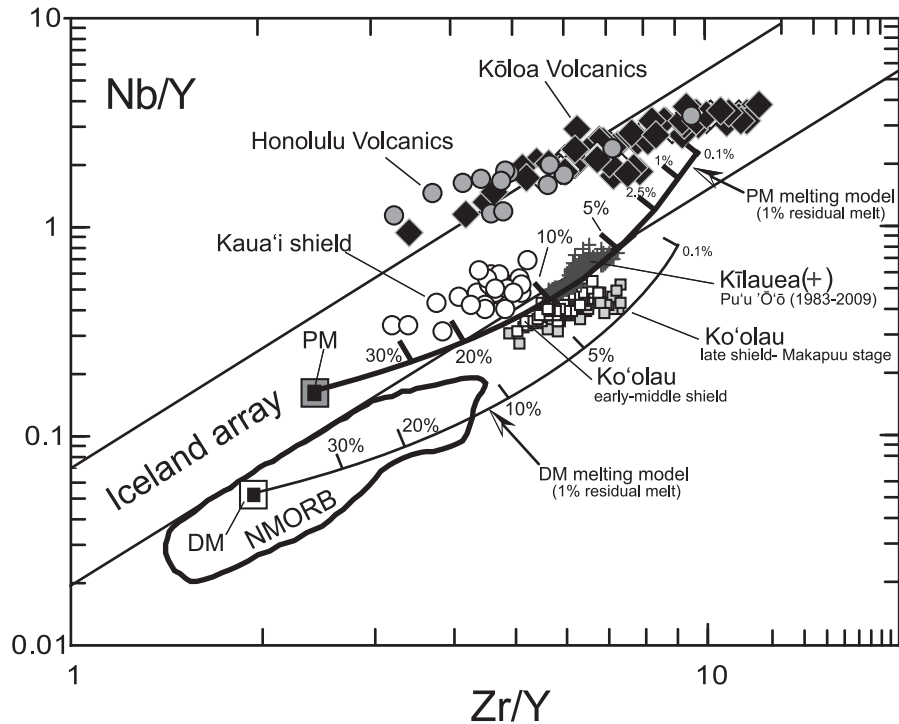The Hawaiian plume is thought to consist of three to four dominant compositional components, although the

Fig. 10. Nb/Y vs Zr/Y for Kōloa Volcanics compared with selected Hawaiian rejuvenated (Honolulu) and shield-stage lavas (Kaua'i, Ko'olau and Kīlauea). Melting model results are shown for primitive mantle (PM) and depleted mantle (DM) with curved lines with tick marks (per cent melting is indicated). The melting models use an incongruent dynamic melting model developed by Zou & Reid (2001). The modeling uses coefficients for incongruent melting reactions based on experiments on lherzolite melting (e.g. Kinzler & Grove, 1992; Longhi, 2002). The models simulated garnet lherzolite melting because garnet is required in the source to reproduce the small variations in HREE observed in Kōloa Volcanics. Source mineralogy for primitive mantle garnet lherzolite is 0·2 cpx, 0·25 opx, 0·5 ol, 0·05 gt, and for depleted mantle garnet lherzolite is 0·09 cpx, 0·2 opx, 0·64 ol, 0·07 gt. The melting models assumed that 1% of the total residue is residual melt. Melt reaction coefficients of garnet lherzolite from Walter (1998). Partition coefficients [from Shaw (2000) and Salters & Stracke (2004)] were kept constant during melting. Data sources: Kōloa Volcanics, this study; Honolulu Volcanics, Yang *et al.* (2003); Kaua'i shield, Mukhopadhyay *et al.* (2003); Kīlauea–Pu'u 'Ō'ō, Garcia *et al.* (1992, 1996, 2000, and unpublished data); Ko'olau shield Kalihi stage, Haskins & Garcia (2004); Ko'olau Makapu'u stage, Frey *et al.* (1994). Diagram originated from Fitton *et al.* (1997). PM, primitive mantle; DM, depleted MORB mantle. PM composition from McDonough & Sun (1995); DM from Salters & Stracke (2004).

identity of these components is hotly debated (e.g. Staudigel *et al.*, 1984; Mukhopadhyay *et al.*, 2003; Frey *et al.*, 2005; Ren *et al.*, 2006, 2009; Tanaka *et al.*, 2008). We seek to evaluate the temporal evolution in the isotopic and trace element composition at one location along the Hawaiian chain for volcanic activity spanning ∼4·5 Myr, the longest timespan in the chain (Fig. 2). To facilitate the discussion of Kaua'i, we consider the variation of three geochemically distinct, Hawaiian plume end-members: Ko'olau (Loa), Kea and DM. Another commonly invoked component, Lō'ihi, is largely recognized based on high He isotope values (Kurz *et al.*, 1983; Ren *et al.*, 2009), which were not determined in this study. In addition, the Ko'olau component has been subdivided by Tanaka *et al.* (2002, 2008) into depleted and enriched components. These other Hawaiian components and ancient depleted mantle are shown in Fig. 6. We use the enriched Ko'olau

component as the end-member of the Loa component, although this component was thought by some to have emerged in the Hawaiian plume at ∼3·0 Ma (Abouchami *et al.*, 2005; Tanaka *et al.*, 2008), after growth of the Kaua'i shield. However, Mukhopadhyay *et al.* (2003) proposed 16–27% Ko'olau component in Kaua'i shield lavas. The DM component is considered to be part of the plume (e.g. Frey *et al.*, 2005) and not MORB-source DM.

The overall temporal evolution in Kaua'i isotopic ratios during the last 4·5 Myr may be explained by varying mixtures of Kea, Ko'olau and DM components. Shield lavas represent a mixture of mostly Kea and Ko'olau components, plotting near the middle of the Hawaiian shield array defined by these two dominant mantle components (Fig. 6). Our new Sr, Nd and Pb isotope data overlap with previous data for the Kaua'i shield (Mukhopadhyay *et al.*,
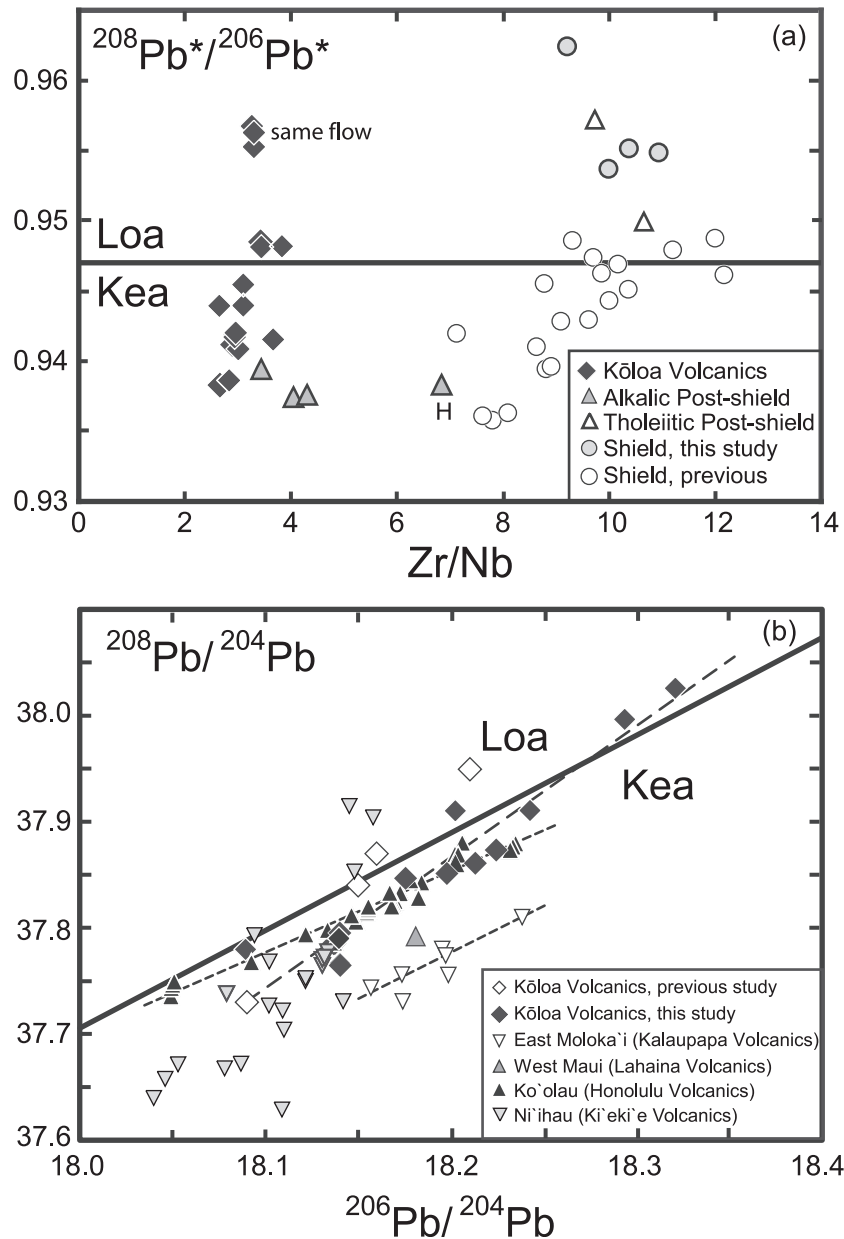
Fig. 11. Comparison of the various stages of Kaua'i volcanism and rejuvenated volcanism from other Hawaiian Islands with the Loa–Kea compositional boundary. (a) $^{208}Pb*/^{206}Pb*$ vs Zr/Nb. $^{208}Pb*/^{206}Pb*$ represents the time-integrated $^{232}Th/^{238}U$ ratio since the formation of the Earth and is defined as: $^{208}Pb*/^{206}Pb* = (^{208}Pb/^{204}Pb - 29{\cdot}475)/(^{206}Pb/^{204}Pb - 9{\cdot}306)$; Galer & O'Nions, 1985). The ratio of $^{208}Pb*/^{206}Pb*$ is radiogenic Pb produced since the formation of the Earth. (b) $^{208}Pb/^{204}Pb$ vs $^{206}Pb/^{204}Pb$. The few Kōloa Volcanics and K'ieki'e Volcanics (Ni'ihau) samples straddle the Loa–Kea boundary line defined by Abouchami et al. (2005), whereas rejuvenated lavas from other islands have Kea-like source. Each rejuvenated lava sequence defines a different high-precision Pb–Pb trend (dashed lines). The scale for $^{206}Pb/^{204}Pb$ is reduced (compared with Fig. 6a) to allow better resolution of the differences among Hawaiian rejuvenated lavas. Data for the Kōloa sample with high Pb isotope values (KR-5, -11 from the same flow with two analyses of KR-5) are not shown. Data for previous Kōloa Volcanics (Lassiter et al., 2000) shown with open diamonds. Kaua'i shield data from Mukhopadhyay et al. (2003); West Maui data from Gaffney et al. (2004); East Moloka'i data from Xu et al. (2005); Honolulu Volcanics data from Fekiacova et al. (2007). Trend lines through the data are shown for each suite of rejuvenated lavas except those from Ni'ihau, which were collected on a TIMS instrument and have a wide scatter (Dixon et al., 2008).

2003), although many of the earlier data plot towards the Kea end-member (i.e. $^{208}Pb*/^{206}Pb* < 0{\cdot}948$) and show a wider range in Sr isotope values (Figs 6 and 11). Previously published data on Kaua'i shield lavas (Reiners & Nelson, 1998; Mukhopadhyay *et al.*, 2003) show an evolution from west to east, with an increase in a $^{208}Pb*/^{206}Pb*$ and $^{87}Sr/^{86}Sr$ and a decrease in ε_{Nd}. Southeast Kaua'i, the area of our shield samples, was not previously sampled. Their isotopic compositions overlap with the literature values for east Kaua'i shield, except in Pb isotope ratios. The dominance of two components is supported by the positive linear trend on an ε_{Hf} vs ε_{Nd} plot for the new tholeiitic shield and post-shield lavas (Fig. 6f). A third component, DM, was invoked to explain the wide range in Sr isotope data at a given $^{206}Pb/^{204}Pb$ value for Kaua'i shield lavas (Mukhopadhyay *et al.*, 2003). Our new Sr isotope data for shield and post-shield tholeiitic lavas do not require this component (Fig. 6). However, Kaua'i alkalic post-shield and rejuvenated lavas exhibit large isotopic variations requiring a depleted source component. This is well shown on plots of Hf and Nd vs Pb isotope ratios, where alkalic samples diverge orthogonally from the arcuate Hawaiian shield trend (Fig. 6b and c).

The correlation of rock type (tholeiitic vs alkali basalt) with isotope composition (Hf, Nd, Sr and $^{208}Pb*/^{206}Pb*$; Table 4; Figs 6 and 11) for coeval post-shield lavas demonstrates that the three dominant source components for the Kaua'i lavas are intimately mixed on a fine scale. The signature of the depleted component is less for the higher degree of melting tholeiitic lavas vs the alkali basalts (Figs 6 and 10). Thus, the extent of melting probably plays a key role in the isotopic composition of the Kaua'i lavas. Other Hawaiian shield volcanoes exhibit the same rock types during the post-shield stage, although their tholeiitic and alkalic lavas are isotopically similar and generally distinct from the shield lavas (e.g. Mauna Kea, Haleakalā, and East Moloka'i; Chen *et al.*, 1991; Kennedy *et al.*, 1991; Xu *et al.*, 2005; Hanano *et al.*, 2010). This shield to post-shield variation in isotopic composition for the younger volcanoes was thought to be related to radial zoning in the Hawaiian plume (e.g. Hauri *et al.*, 1994). The absence of this variation for the Kaua'i tholeiitic lavas suggests radial zoning may be a recent phenomenon for the Hawaiian plume or that another explanation should be sought for the isotopic variation in the younger Hawaiian volcanoes.

The magnitude of Kaua'i's post-shield isotopic variations is similar to that reported for Kīlauea shield lavas erupted over only a few thousand years (Marske *et al.*, 2007). These relatively large isotopic variations over relatively short time periods indicate that the Hawaiian plume is heterogeneous on a small scale. The implications of these results for the structure of the Hawaiian plume are discussed below.

LOA SOURCE COMPONENT IN KAUA'I LAVAS

The Hawaiian plume displays a bilateral asymmetry in radiogenic Pb isotopes for lavas erupted south of the Moloka'i fracture zone on the Loa vs Kea trends (Tatsumoto, 1978; Abouchami *et al.*, 2005). Our new results show that Kaua'i lavas straddle the Loa–Kea Pb isotope boundary (Fig. 11a). These results indicate that the Loa component is more widespread within the Hawaiian plume than previously thought and that its presence is not related to the Moloka'i fracture zone (Abouchami *et al.*, 2005) or plate motion shifts (Xu *et al.*, 2007; Tanaka *et al.*, 2008). No spatial distribution is evident for the Kaua'i shield, post-shield or rejuvenated lavas (Fig. 1) to account for the distribution of Loa and Kea radiogenic Pb isotope values. Also, there is no temporal pattern to the distribution of Loa-type samples. They occur in rocks from all stages of growth of the island with ages ranging from 0·7 to 4·3 Ma, although not consistently (Tables 1 and 4). This is in sharp contrast to dominance of the Loa component in the uppermost shield lavas at Ko'olau (Salters *et al.*, 2006) and West Moloka'i volcanoes (Xu *et al.*, 2007). This temporal variation was used to argue for a bilaterally zoned plume assuming that the Loa component has a relatively low solidus (e.g. Xu *et al.*, 2007). The Kaua'i results appear to be inconsistent with this assumption. The Loa component appears in all six of the tholeiitic samples we analyzed (including the post-shield samples), and is absent in the four post-shield alkalic and most extreme rejuvenation stage samples (Fig. 11). The presence of the Loa component during the post-shield stage only in the tholeiites argues that it is unlikely to be the component with the lowest melting temperature in the Hawaiian plume.

The persistence of the Loa component in all stages of volcanism on Kaua'i suggests that the Loa component is well mixed within the Hawaiian plume, and there is no need to invoke a change in melting conditions or shift in the thermal axis of the plume. This interpretation agrees with the recognition of both Kea and Loa components in tholeiitic lavas from other Hawaiian volcanoes (Haleakalā, Ren *et al.*, 2006; Kīlauea, Marske *et al.*, 2008). These results also indicate that both Loa and Kea components were present within the Hawaiian plume at 4·3 Ma, rather than appearing at >3 Ma. Evaluating the longevity of the Loa component and its origin within the plume is beyond the scope of this study. It will require geochemical work on volcanoes to the NW of Kaua'i along the Hawaiian Ridge to evaluate the extent of the Loa component in the Hawaiian plume.

Among other Hawaiian rejuvenated sequences, those erupted on and around the neighboring island of Ni'ihau (Ki'eki'e Volcanics), also plot on both sides of the Kea–Loa line (Fig. 11b). This was not recognized previously. The Ni'ihau and Kaua'i rejuvenated lavas are coeval (Sherrod

et al., 2007). In contrast, all rejuvenated lavas on younger Hawaiian shield volcanoes plot only on the Kea side of the line (Fig. 11b) even though most erupted during the same time interval as the Kōloa lavas (Fig. 2) and they occur in both the Loa- and Kea-type volcanoes (Fig. 6). Thus, rejuvenated lavas have been derived from both Kea and Loa source components, although none of the rejuvenated lavas erupted south of Kaua'i have both components. The implications of the Loa component in Kaua'i and Ni'ihau rejuvenated lavas will be examined in the plume structure section below.

GEOCHEMICAL EVOLUTION OF KAUA'I: IMPLICATIONS FOR PLUME STRUCTURE

The isotopic and trace element evidence that Kōloa (Figs 6 and 10) and other rejuvenated lavas (Frey *et al.*, 2005; Fekiacova *et al.*, 2007) are derived from the Hawaiian plume rather than the lithosphere allows us to examine the plume's evolution over ∼4·5 Myr at one location. An alternative and complementary approach examined the isotopic variation along the Hawaiian chain over 5 Myr for shield volcanoes (Tanaka *et al.*, 2008). We include rejuvenated lavas in our evaluation of the temporal evolution of Kaua'i to gain a better understanding of the DM component distribution within the Hawaiian plume and to evaluate models for the origin of the rejuvenated volcanism.

Two basic models have been proposed for the geochemical structure of the Hawaiian plume: (1) radial zoning (e.g. Hauri *et al.*, 1996; Lassiter *et al.*, 1996; Blichert-Toft *et al.*, 2003; Bryce *et al.*, 2005); (2) bilateral asymmetry with vertically stretched isotopically heterogeneous 'filaments' (Abouchami *et al.*, 2005). Neither of these models adequately explains the geochemical trends seen in all Hawaiian shield lavas without invoking small-scale, time-varying blob and/or string-shaped heterogeneities (e.g. Garcia *et al.*, 2000; Mukhopadhyay *et al.*, 2003; Ren *et al.*, 2005; Marske *et al.*, 2007). The 4·5 Ma Kaua'i isotopic record of magmatism provides additional justification for revising the simple lateral or radial zonation plume models.

The contribution of the DM component was highly variable during Kaua'i volcanism (Fig. 6), although overall it increased with time. During the Kaua'i's post-shield alkalic phase (3·9–3·6 Ma), Hf and Nd isotope ratios increased and $^{87}Sr/^{86}Sr$ values decreased, indicating the emergence of the DM component (Figs 6 and 11). The greater proportion of the DM component in the rejuvenated lavas, which are formed at low degrees of melting (e.g. Clague & Frey, 1982), suggests that this component has been recently enriched (necessary to prevent the

isotopic ratios from changing), lowering its solidus temperature.

The increased involvement of the DM component in the younger Kaua'i lavas may be related to the drift of the island off the plume axis, a decrease in the extent of partial melting during the post-shield and rejuvenation stages (3·9–0·15 Ma) or a switch in mechanism for melt generation. Isotopic and seismic evidence (Woods *et al.*, 1991; Fekiacova *et al.*, 2007) and numerical modeling of the plume–lithosphere interaction (Ribe & Christensen, 1999) have been used to suggest that the DM component is entrained by the upwelling plume (Mukhopadhyay *et al.*, 2003; Fekiacova *et al.*, 2007). However, other studies have suggested that this switch in source components is a consequence of melting a heterogeneous source (i.e. different components of the plume contribute at different stages, with the most depleted component appearing later because of its more refractory nature; e.g. Bianco *et al.*, 2005; Paul *et al.*, 2005). All of these factors are consistent with available data and may contribute to the source change.

The Pb, Nd, Hf and Sr isotopic data are consistent with the involvement of the Kea component in each stage of Kaua'i's eruptive history (Fig. 6) and for most Hawaiian volcanoes (Tanaka *et al.*, 2008). Thus, this component most probably forms the matrix of the Hawaiian plume (Fig. 12). Alternatively, the Kea component may be the lowest melting temperature component. Other source components sampled by Hawaiian volcanoes (Ko'olau and DM) are evidently present as much smaller domains in the plume (blobs and/or strings) and are relatively short-lived or swamped by the Kea component at higher degrees of partial melting, except on the west side of the Hawaiian paired sequence where it is the probably the dominant component (e.g. Hauri, 1996; Abouchami *et al.*, 2005). A heterogeneous plume model (Fig. 12) is a viable alternative to the radially zoned or bilaterally zoned plume models for explaining the presence of multiple components in magmas from each volcanic stage.

IMPLICATIONS OF VOLUMES, AGES AND GEOCHEMISTRY FOR REJUVENATED VOLCANISM MODELS

The current causation models for rejuvenated volcanism are: (1) lithospheric melting by conductive heating (Gurriet, 1987); (2) a second zone of mantle plume melting (Ribe & Christensen, 1999); (3) flexure-induced decompressional melting (Jackson & Wright, 1970; Bianco *et al.*, 2005). These models were designed to explain the generation of alkalic magmas by low degrees of partial melting, a characteristic feature of rejuvenated volcanism (e.g. Clague & Frey, 1982). These models make predictions about the length of the volcanic hiatus between the
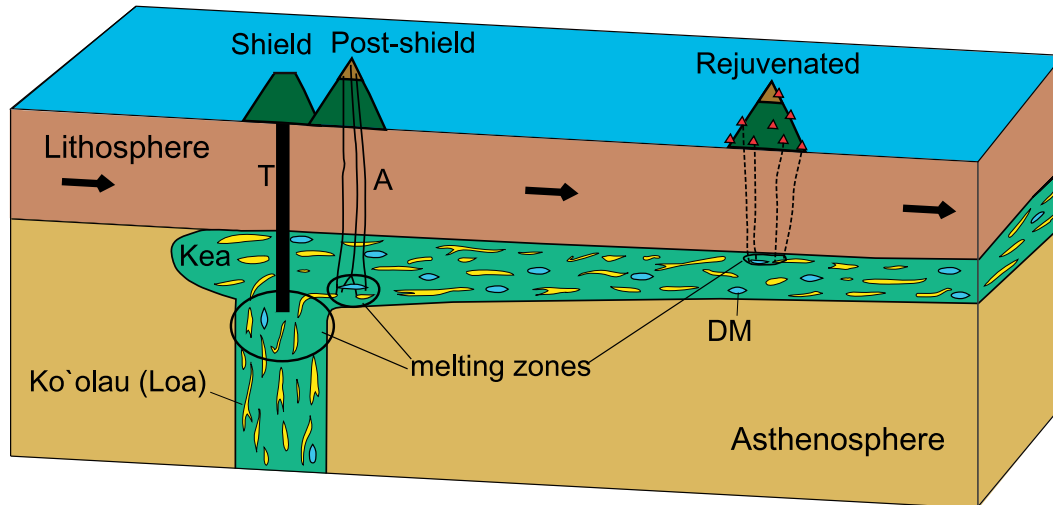
Fig. 12. Schematic illustration of the plume structure during the 5 Myr evolution of Kaua'i from shield to rejuvenated stage. The vertical plume stem consists of rapidly upwelling material from the deep mantle. The plume spreads out laterally and rises as it is dragged beneath the migrating ~100 km thick Pacific lithosphere. The plume consists of a matrix containing the Kea component, with 'blobs' of the Ko'olau and DM components. The shield stage of Kaua'i incorporates Kea and Ko'olau components with little or no DM material. The post-shield lavas form as Kaua'i moves away from the vertical plume stem. The rejuvenated volcanism occurs 300–400 km downstream from the vertical plume stem, incorporating a greater contribution from the DM plus a mixture of Kea and Ko'olau components. The greater proportion of DM component in the rejuvenated lavas, which are formed at low degrees of melting (e.g. Clague & Frey, 1982), suggests that this component has been recently enriched, lowering its solidus temperature.

Table 6: Comparison of predicted estimates for magma volume and flux rates, hiatus and volcanism durations, and magma sources vs observed values for Kōloa Volcanics

Mechanism	Volume, flux rate (km^3, km^3/Myr)	Hiatus duration (Myr)	Volcanism duration (Myr)	Source
Conductive heating (Gurriet, 1987)	<100, <100	short (<0·5) or none	long (~5)	lithosphere
Secondary plume (Ribe & Christensen, 1999)	10–20, 10	1–2	2–3	plume
Flexure induced (Bianco *et al.*, 2005)	10–18, 13	0·85–1·75	1·5–2·25	plume
Kāloa Volcanics (this study)	58, 24	1·0	2·45	plume

Estimates compiled from sources as noted under mechanism.

post-shield and rejuvenated volcanism (in Myr), the duration of volcanism (Myr), melt volume flux (km^3/Myr) and the nature of the source. We have summarized these variables for the current models in Table 6. These predictions are now testable using our new results for the volume, geochronology and geochemistry of the Kōloa lavas.

None of the three models above satisfactorily explains the observed features of the Kōloa Volcanics (Table 6). The lithospheric melting by conductive heating model advocates melting of the lower lithosphere (Gurriet, 1987). This is inconsistent with the new Pb isotope data for both the Kōloa (Fig. 6) and Honolulu Volcanics (Fekiacova *et al.*, 2007) and the trace element data (Fig. 10). This model also fails to explain the ~1 Myr hiatus in Kaua'i's volcanism following the shield stage (Fig. 2). The secondary zone of mantle plume melting and flexure-induced decompression melting models both advocate a plume source. Therefore, additional criteria, such as rock type and age distribution, and geochemical and isotopic data, are required
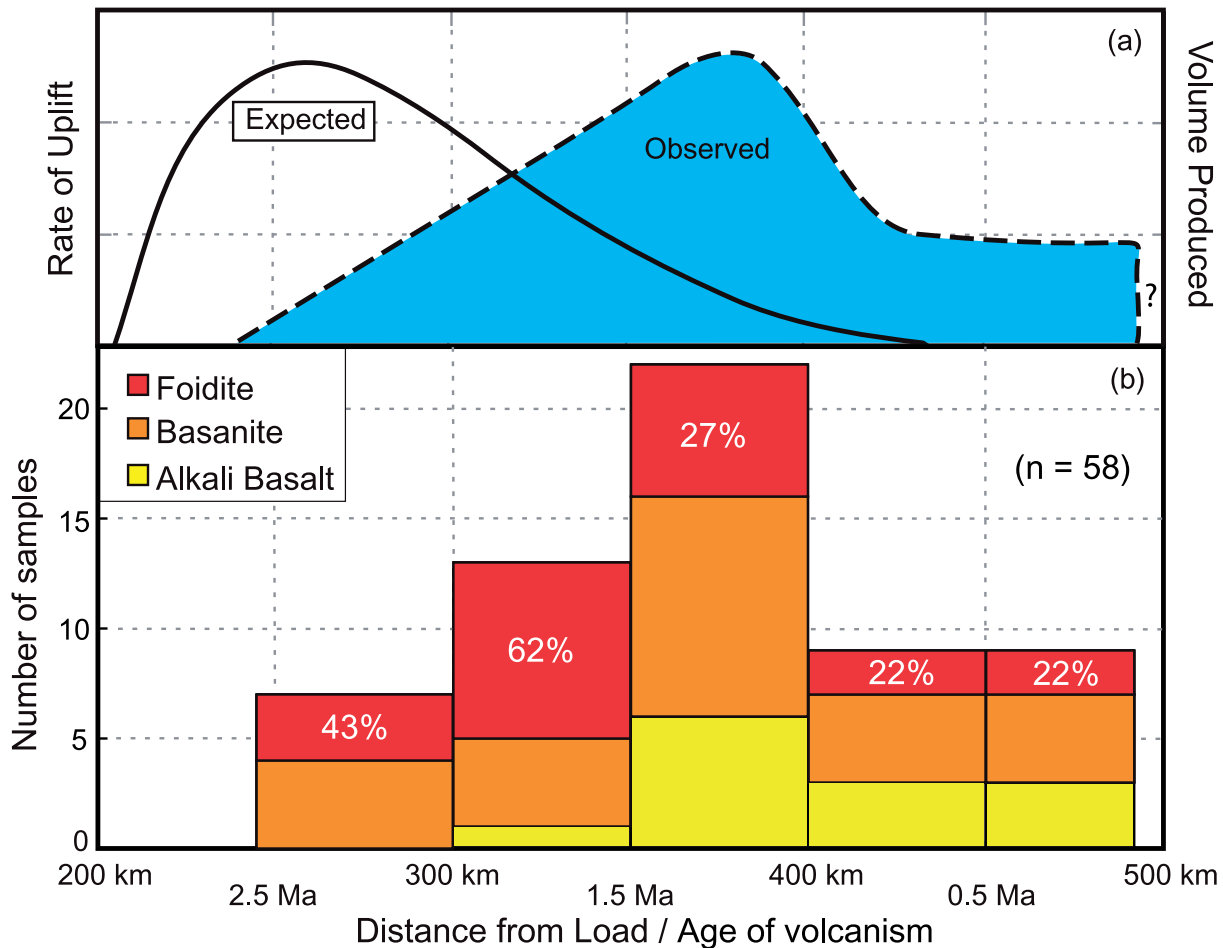
Fig. 13. (a) Qualitative representation of the temporal variation in predicted rate of flexural uplift (equivalent to magma flux rate) from the loading of the Pacific plate by new Hawaiian shield volcanism (from Bianco *et al.*, 2005). The *y*-axis indicates relative intensity of predicted melt generation, which is plotted against observed eruption rate (based on new and previous radiometric ages). Kaua'i is ∼500 km from the load focus near Mauna Loa volcano. The Pacific plate is assumed to have moved NW at a rate of ∼100 km/Myr (Garcia *et al.*, 1987). Kōloa volcanism began ∼0·3 Myr later than expected and continued for ∼0·5 Myr longer than predicted. (b) Histogram of rock types vs age in 0·5 Ma bins. Oldest rocks are strongly alkalic, foidites and basanites (there are no alkali basalts). A peak in volcanism occurs at the midpoint of the duration of rejuvenated volcanism on Kaua'i, producing all three rock types. Volcanism apparently decreased markedly during the last 1 Myr, although it was not accompanied by an increase in percentage of foidites (shown in boxes). Age data from McDougall (1964), Clague & Dalrymple (1988), Hearty *et al.* (2005) and Table 1.

to evaluate these models. The secondary zone of mantle plume melting model generates a much smaller volume and lower magma flux rate for the rejuvenated volcanism than observed on Kaua'i (10–20 km^3, 10 km^3/Myr vs 58 km^3, 24 km^3/Myr observed; Table 6). Also, our modeling of the depth of melting for the rejuvenated magmas places it near the top of the plume (Fig. 12) rather than at the base as indicated by the secondary melting model (3·5–4 vs 5–6 GPa; Ribe & Christensen, 1999).

The flexure-induced decompression melting model of Bianco *et al.* (2005) has greater predictive capabilities for rejuvenated volcanism allowing us to compare it with observed features. For example, the flexure model predicts the duration and timing of rejuvenated volcanism based

on the load over the plume stem (Bianco *et al.*, 2005). Comparing model predictions with the 57 K–Ar dated Kōloa lavas reveals a broadly similar frequency pattern (Fig. 13). However, there are several critical inconsistencies: the peak in Kōloa volcanism is much younger than expected (1·0–1·5 Ma observed vs 2·0–2·5 Ma predicted); volcanism should have ended when Kaua'i stopped uplifting at ∼0·75 Ma rather than persisting until at least 0·15 Ma; and there is no apparent decline in activity during the last 1 Myr (Fig. 13). Also, the flexure model predicts a lower volume and flux rate than observed (10–18 km^3, 13 km^3/Myr for the flexure model vs 58 km^3, 24 km^3/Myr observed; Table 6). The flexure model also fails to explain the observed simultaneous rejuvenated

volcanism along a 350 km segment of the Hawaiian chain (from the islands of Maui to Ni'ihau at 0·35–0·6 Ma; Fig. 2).

The flexural model can be used to infer temporal variations in magma compositions based on the amount of flexural uplift, which controls the per cent of melting (Bianco *et al.*, 2005) and the magma major element composition (e.g. Clague & Frey, 1982). Early and late stages of rejuvenated volcanism should be dominated by minor uplift and low degrees of melting producing foidites, whereas the main pulse of volcanism should result from higher degrees of partial melting producing alkali basalts and basanites. This pattern is well reflected in the early period (>1·5 Ma) of Kōloa volcanism (~40–60% foidites and 0–10% alkali basalts), changing to nearly equal proportions of foidites and alkali basalts during the main pulse of melting (Fig. 13). An opposite pattern was observed for drill core from the Lihue basin (Reiners & Nelson, 1998), which formed during the peak of rejuvenated volcanism (1·2–1·5 Ma, Fig. 13). However, during the latter stages of Kōloa volcanism (<1 Ma) when the extent of partial melting should have decreased, the abundance of foidites apparently decreases slightly and alkali basalts actually increase. This is opposite to the expected rock type variation.

Our new geochemical and geochronological data for Kōloa lavas show a delayed start for and an extended duration of the volcanism, a relatively shallow Hawaiian plume source, a voluminous and high flux rate of volcanism and temporal variation in rock types (Fig. 13), plus the presence of synchronous rejuvenated volcanism along 350 km of the Hawaiian chain (Fig. 2). These features are inconsistent with all of the current models for this volcanism. However, combining the two plume source models (lithospheric flexure and secondary zone of melting) provides a physical mechanism to initiate rejuvenated volcanism and to focus the melting at shallower levels within the plume (lithospheric flexural uplift), with a method to extend the duration of Kōloa volcanism at higher degrees of partial melting (secondary zone of plume uplift). This hybrid scenario should be examined further by numerical modeling.

CONCLUSIONS

Kaua'i lavas provide a unique opportunity to evaluate 4·5 Myr of Hawaiian plume magmatic activity at one location. Our study of these lavas has led to the following interpretations.

(1) Combining new and previous geochronology results indicates that the Kaua'i subaerial shield stage volcanism occurred from >5·1 to 4·0 Ma. Post-shield tholeiitic and alkalic lavas were erupted from 3·95 to 3·6 Ma. A 1 Myr gap separates the end of this volcanism from the onset of rejuvenated stage volcanism,

which was active from 2·6 to 0·15 Ma. Thus, the Kaua'i rejuvenated stage lasted for at least 2·45 Myr, the longest Hawaiian example.

(2) The volume of the rejuvenated stage of volcanism on Kaua'i is estimated at 58 km³, about 0·1% of the total island edifice volume. This is the first quantitative estimate for the rejuvenation stage on any Hawaiian island. Using the new ages, the average flux rate for Kaua'i rejuvenated volcanism was 24 km³/Myr, much higher than predicted by some models.

(3) Tholeiitic shield and post-shield lavas are geochemically and isotopically similar but are distinct from coeval alkalic post-shield and later rejuvenated lavas. Thus, during the post-shield stage, the extent of melting plays a critical role in determining which source dominates the isotopic signature of the lavas.

(4) Modeling of major elements for four weakly alkalic Kaua'i rejuvenated lava compositions using the PRIMELT2 program indicates that they formed by low-degree melting (0·02–2·6%) at high temperatures and pressures (~1525 ± 10°C and 3·5–4·0 GPa) of a peridotitic plume source.

(5) Three components within the Hawaiian plume, Kea, Ko'olau (Loa) and ancient depleted mantle (DM), are primarily responsible for most of the Pb, Hf, Sr and Nd isotopic variation in the Kaua'i lavas. Shield and tholeiitic post-shield volcanism involved a Loa component. The depleted mantle is a long-term and integral part of the Hawaiian plume, appearing during all stages of Hawaiian volcanism, although it is mainly sampled during lower degrees of melting at the end of shield volcanism and during the rejuvenated volcanism.

(6) The Loa component is observed in all stages of Kaua'i volcanism, spanning 4·1 Myr. Thus, this component is pervasive and long-lived in the Hawaiian plume. Its dominance in Kaua'i tholeiites suggests that it is not necessarily a lower melting component of the plume, as suggested by previous workers. The presence of the Ko'olau component in the Kaua'i lavas invalidates current models for the origin of this component in the Hawaiian plume. More work is needed to the north of Kaua'i to determine the regional extent of this component before we can determine its origin.

(7) Isotopic and trace element data show that the Kaua'i (and probably other) rejuvenated lavas have no genetic relationship with Pacific lithosphere, as sampled by xenoliths from Hawaiian volcanoes, and MORB samples collected near Hawai'i at ODP Site 843 and from the East Pacific Rise. Thus, lithospheric melting is unlikely to account for the production of the rejuvenated stage magmas in Hawai'i, nor can it explain the 1 Myr gap in volcanism on Kaua'i.

(8) The other two models for rejuvenated volcanism, flexural uplift and secondary zone of melting, do not explain the ages, rock types and geochemistry of the Hawaiian rejuvenated volcanism. The large volume and high flux rate, and the relatively shallow depth of melting inferred from major element modeling, are incompatible with the secondary zone of melting model. The long duration and overall timing, large volume and high flux rate, rock type temporal variation, and synchronous rejuvenated volcanism along a 350 km long section of the Hawaiian chain are contrary to the predictions of the flexural uplift melting model. If lithospheric flexure and secondary zone of melting models are combined, however, they provide a physical mechanism to initiate rejuvenated volcanism and to focus the melting at shallower levels within the plume (flexural uplift), with a process to extend the duration of Kōloa volcanism at higher degrees of partial melting (secondary zone of plume uplift).

SUPPLEMENTARY DATA

Supplementary data for this paper are available at *Journal of Petrology* online.

REFERENCES

Abouchami, W., Galer, S. J. G. & Hofmann, A. W. (2000). High precision lead isotope systematics of lavas from the Hawaiian Scientific Drilling Project. *Chemical Geology* **169**, 187–209.

Abouchami, W., Hofmann, A. W., Galer, S. J. G., Frey, F. A., Eisele, J. & Feigenson, M. (2005). Lead isotopes reveal bilateral asymmetry and vertical continuity in the Hawaiian mantle plume. *Nature* **434**, 851–856.

Bianco, T. A., Ito, G., Becker, J. M. & Garcia, M. O. (2005). Secondary Hawaiian volcanism formed by flexural arch decompression. *Geochemistry, Geophysics, Geosystems* **6**, 2005GC000945.

Blichert-Toft, J. & White, W. M. (2001). Hf isotope geochemistry of the Galapagos Islands. *Geochemistry, Geophysics, Geosystems* **2**, 2000GC000138.

Blichert-Toft, J., Frey, F. A. & Albarède, F. (1999). Hf isotope evidence for pelagic sediments in the source of Hawaiian basalts. *Science* **285**, 879–882.

Blichert-Toft, J., Weis, D., Maerschalk, C., Agranier, A. & Albarède, F. (2003). Hawaiian hot spot dynamics as inferred from the Hf and Pb isotope evolution of Mauna Kea volcano. *Geochemistry, Geophysics, Geosystems* **4**, 2002GC00340.

Bryce, J. G., DePaolo, D. J. & Lassiter, J. C. (2005). Geochemical structure of the Hawaiian plume: Sr, Nd and Os isotopes in the 2·8 km HSDP-2 section of Mauna Kea volcano. *Geochemistry, Geophysics, Geosystems* **6**, 2004GC000809.

Castillo, P., Klein, E., Bender, J., Langmuir, C., Shirley, S., Batiza, R. & White, W. (2000). Petrology and Sr, Nd, and Pb isotope geochemistry of mid-ocean ridge basalt glasses from the 11°45′N to 15°00′N segment of the East Pacific Rise. *Geochemistry, Geophysics, Geosystems* **1(11)**, doi:10.1029/1999GC000024.

Chauvel, C. & Blichert-Toft, J. (2001). A hafnium isotope and trace element perspective on melting of the depleted mantle. *Earth and Planetary Science Letters* **190**, 137–151.

Chen, C.-Y., Frey, F. A., Garcia, M. O., Dalrymple, G. B. & Hart, S. R. (1991). The tholeiite to alkalic basalt transition at Haleakala Volcano, Maui, Hawaii. *Contributions to Mineralogy and Petrology* **106**, 183–200.

Chen, C.-Y., Frey, F. A., Rhodes, J. M. & Easton, R. M. (1996). Temporal geochemical evolution of Kīlauea volcano: comparison of Hilina and Puna basalt. In: Basu, A. & Hart, S. (eds) *Earth Processes: Reading the Isotopic Code. Geophysical Monograph, American Geophysical Union* **95**, 161–181.

Clague, D. A. & Dalrymple, G. B. (1988). Age and petrology of alkalic postshield and rejuvenated-stage lava from Kauai, Hawaii. *Contributions to Mineralogy and Petrology* **99**, 202–218.

Clague, D. A. & Frey, F. A. (1982). Petrology and trace element geochemistry of the Honolulu Volcanics, Oahu; implications for the oceanic mantle below Hawaii. *Journal of Petrology* **23**, 447–504.

Clague, D. A., Dao-gong, C., Murnane, R., Beeson, M. H., Lanphere, M. A., Dalrymple, B., Friesen, W. & Holcomb, R. T. (1982). Age and petrology of Kalaupapa basalt, Molokai, Hawaii. *Pacific Science* **36**, 411–420.

Clague, D. A., Cousens, B. L., Davis, A. S., Dixon, J. E., Hon, K., Moore, J. G. & Reynolds, J. R. (2003). Rejuvenated-stage lavas offshore Molokai, Oahu, Kaua'i, and Niihau, Hawaii. *EOS Transactions, American Geophysical Union* **84**, V11B–01.

Connelly, J. N., Ulfbeck, D. G., Thrane, K., Bizzarro, M. & Housh, T. (2006). A method for purifying Lu and Hf for analyses by MC-ICP-MS using TODGA resin. *Chemical Geology* **233**, 126–136.

Dasgupta, R., Hirschmann, M. M. & Smith, N. D. (2007). Partial melting experiments of peridotite + CO_2 at 3 GPa and genesis of alkalic ocean island basalts. *Journal of Petrology* **48**, 2093–2124.

Dixon, J., Clague, D. A., Cousens, B., Monsalve, M. L. & Uhl, J. (2008). Carbonatite and silicate melt metasomatism of the mantle surrounding the Hawaiian plume: Evidence from volatiles, trace elements and radiogenic isotopes in rejuvenated-stage lavas from Niihau, Hawii. *Geochemisry, Geophysics, Geosystems* **9**, Q09005, doi:10.1029/2008GC002076.

Doucet, S., Weis, D., Scoates, J. S., Nicolaysen, K., Frey, F. A. & Giret, A. (2002). The depleted mantle component in Kerguelen Archipelago basalts: Petrogenesis of tholeiitic–transitional basalts from the Loranchet Peninsula. *Journal of Petrology* **43**, 1341–1366.

Duncan, R., Fisk, M., White, W. M. & Nielsen, R. L. (1994). Tahiti: Geochemical evolution of a French Polynesian volcano. *Journal of Geophysical Research* **99**, 24341–24357.

Environmental Systems Research Institute. (2004). *ArcGIS 9: Using ArcMap.* New York: ESRI, 585 p.

Feigenson, M. D. (1984). Geochemistry of Kauai volcanics and a mixing model for the origin of Hawaiian alkali basalts. *Contributions to Mineralogy and Petrology* **87**, 109–119.

Fekiacova, Z., Abouchami, W., Galer, S. J. G., Garcia, M. O. & Hofmann, A. W. (2007). Temporal evolution of Ko'olau Volcano: inferences from isotope results on the Ko'olau Scientific Drilling Project (KSDP) and Honolulu Volcanics. *Earth and Planetary Science Letters* **261**, 65–83.

Fitton, J. G., Saunders, A. D., Norry, M. J., Hardarson, B. S. & Taylor, R. N. (1997). Thermal and chemical structure of the Iceland plume. *Earth and Planetary Science Letters* **153**, 197–208.

Fodor, R. V., Frey, F. A., Bauer, G. R. & Clague, D. A. (1992). Ages, rare-earth element enrichment, and petrogensis of tholeiitic and alkalic basalts from Kaho'olawe Island, Hawaii. *Contributions to Mineralogy and Petrology* **110**, 442–462.

Frey, F. A., Garcia, M. O., Wise, W. S., Kennedy, A., Gurriet, P. & Albarède, F. (1991). The evolution of Mauna Kea Volcano, Hawaii: Petrogenesis of tholeiitic and alkalic basalts. *Journal of Geophysical Research* **96**, 14347–14375.

Frey, F. A., Garcia, M. O. & Roden, M. F. (1994). Geochemical characteristics of Ko'olau Volcano: implications of intershield geochemical differences among Hawaiian volcanoes. *Geochimica et Cosmochimica Acta* **58**, 1441–1462.

Frey, F. A., Huang, S., Blichert-Toft, J., Regelous, M. & Boyet, M. (2005). Origin of depleted components in basalt related to the Hawaiian hot spot: Evidence from isotopic and incompatible element ratios. *Geochemistry, Geophysics, Geosystems* **6**, 2004GC000757.

Gaffney, A. M., Nelson, B. K. & Blichert-Toft, J. (2004). Geochemical constraints on the role of oceanic lithosphere in intra-volcano heterogeneity at West Maui, Hawaii. *Journal of Petrology* **45**, 1663–1687.

Gaffney, A. M., Nelson, B. K. & Blichert-Toft, J. (2005). Melting in the Hawaiian plume at 1–2 Ma as recorded at Maui Nui: the role of eclogite, peridotite, and source mixing. *Geochemistry, Geophysics, Geosystems* **6**, 2005GC000927.

Galer, S. J. G. & O'Nions, R. K. (1985). Residence time of thorium, uranium and lead in the mantle with implications for mantle convection. *Nature* **316**, 778–782.

Garcia, M. O., Grooms, D. G. & Naughton, J. J. (1987). Petrology and geochronology of volcanic rocks from seamounts along and near the Hawaiian Ridge; implications for propagation rate of the ridge. *Lithos* **20**, 323–336.

Garcia, M. O., Rhodes, J. M., Wolfe, E. W., Ulrich, G. E. & Ho, R. A. (1992). Petrology of lavas from episodes 2–47 of the Pu'u 'Ō'ō eruption of Kīlauea Volcano, Hawaii: Evaluation of magmatic processes. *Bulletin of Volcanology* **55(1)**, 1–16.

Garcia, M. O., Foss, D., West, H. & Mahoney, J. (1995). Geochemical and isotopic evolution of Loihi Volcano, Hawaii. *Journal of Petrology* **36**, 1647–1674.

Garcia, M. O., Rhodes, J. M., Trusdell, F. A. & Pietruszka, A. J. (1996). Petrology of lavas from the Pu'u 'Ō'ō eruption of Kīlauea Volcano: III The Kupaianaha episode (1986–1992). *Bulletin of Volcanology* **58**, 359–379.

Garcia, M. O., Pietruszka, A. J., Rhodes, J. M. & Swanson, K. (2000). Magmatic processes during the prolonged Pu'u 'O'o eruption of Kīlauea Volcano, Hawaii. *Journal of Petrology* **41**, 967–990.

Garcia, M. O., Ito, G., Weis, D. *et al.* (2008). Widespread secondary volcanism around the northern Hawaiian Islands. *EOS Transactions, American Geophysical Union* **52**, 542–543.

Geldmacher, J. & Hoernle, K. (2000). The 72 Ma geochemical evolution of Madeira hotspot: recycling of Paleozoic (<500 Ma) oceanic lithosphere. *Earth and Planetary Science Letters* **183**, 73–92.

Geldmacher, J., Hoernle, K., Bogaard, P.v.d., Duggen, S. & Werner, R. (2005). New $^{40}Ar/^{39}Ar$ age and geochemical data from seamounts in the Canary and Madeira volcanic provinces: support for the mantle plume hypothesis. *Earth and Planetary Science Letters* **237**, 85–101.

Gurenko, A. A., Hoernle, K. A., Sobolev, A. V., Hauff, F. & Schmincke, H.-U. (2010). Source components of the Gran Canaria shield stage magmas. *Contributions to Mineralogy and Petrology* **159**, 689–702.

Gurriet, P. (1987). A thermal model for the origin of post-erosional alkalic lava, Hawaii. *Earth and Planetary Science Letters* **82**, 153–158.

Hanan, B. B., Blichert-Toft, J., Kingsley, R. & Schilling, J. G. (2000). Depleted Iceland mantle plume geochemical signature: Artifact of multicomponent mixing? *Geochemistry, Geophysics, Geosystems* **1(Q01003)**, doi:10.1029/1999GC000009.

Hanano, D., Weis, D., Scoates, J. S., Aciego, S. & DePaolo, D. J. (2010). Horizontal and vertical zoning of heterogeneities in the Hawaiian mantle plume from the geochemistry of consecutive post-shield volcano pairs: Kohala–Mahukona and Mauna Kea–Hualalai. *Geochemistry, Geophysics, Geosystems* **11(Q01004)**, doi:10.1029/2009GC002782.

Haskins, E. H. & Garcia, M. O. (2004). Scientific drilling reveals geochemical heterogeneity within the Ko'olau Shield, Hawai'i. *Contributions to Mineralogy and Petrology* **147**, 162–188.

Hauri, E. H. (1996). Major-element variability in the Hawaiian mantle plume. *Nature* **382**, 415–419.

Hauri, E. H., Whitehead, J. A. & Hart, S. R. (1994). Fluid dynamic and geochemical aspects of entrainment in mantle plumes. *Journal of Geophysical Research* **99**, 24275–24300.

Hearty, P. J., Karner, D. B., Renne, P. R., Olson, S. L. & Fletcher, S. (2005). $^{40}Ar/^{39}Ar$ age of a young rejuvenation basalt flow: implications for the duration of volcanism and the timing of carbonate platform development during the Quaternary on Kaua'i, Hawaiian Islands. *New Zealand Journal of Geology and Geophysics* **48**, 199–211.

Herzberg, C. (2006). Petrology and thermal structure of the Hawaiian plume from Mauna Kea volcano. *Nature* **444(7119)**, 605.

Herzberg, C. & Asimow, P. D. (2008). Petrology of some oceanic island basalts: PRIMELT2.XLS software for primary magma calculation. *Geochemistry, Geophysics, Geosystems* **9(Q09001)**, doi:10.1029/2008GC002057.

Herzberg, C. & Gazel, E. (2009). Petrological evidence for secular cooling in mantle plumes. *Nature* **458(7238)**, 619–622.

Herzberg, C. & O'Hara, M. J. (2002). Plume-associated ultramafic magmas of Phanerozoic age. *Journal of Petrology* **43(10)**, 1857–1883.

Herzberg, C., Asimow, P. D., Arndt, N., Niu, Y., Lesher, C. M., Fitton, J. G., Cheadle, M. J. & Saunders, A. D. (2007). Temperatures in ambient mantle and plumes: Constraints from basalts, picrites, and komatiites. *Geochemistry, Geophysics, Geosystems* **8(Q02006)**, doi:10.1029/2006GC001390.

Hoernle, K. & Schmincke, H.-U. (1993). The petrology of the tholeiites through melilite nephelinites on Gran Canaria, Canary Islands; crystal fractionation, accumulation, and depths of melting. *Journal of Petrology* **34**, 573–597.

Hoernle, K., Tilton, G. E., Le Bas, M. J., Duggan, S. & Garbe-Schoonberg, D. (2002). Geochemistry of oceanic carbonatites compared with continental carbonatites: mantle recycling of oceanic crustal carbonate. *Contributions to Mineralogy and Petrology* **142**, 520–542.

Holm, P. M., Wilson, J. R., Christensen, B. P., Hansen, L., Hansen, S. L., Hein, K. M., Mortensen, A. K., Pedersen, R., Plesner, S. & Runge, M. K. (2006). Sampling the Cape Verde mantle plume: evolution of melt compositions on Santo Antão, Cape Verde Islands. *Journal of Petrology* **47(1)**, 145–189, doi:10.1093/petrology/egi071.

Huang, S., Frey, F. A., Blichert-Toft, J., Fodor, R. V., Bauer, G. R. & Xu, G. (2005). Enriched components in the Hawaiian plume: evidence from Kaho'olawe Volcano, Hawaii. *Geochemistry, Geophysics, Geosystems* **6**, 2005GC001012.

Izuka, S. K. (2006). Effects of Irrigation, Drought, and Ground-Water Withdrawals on Ground-Water Levels in the Southern Lihue Basin, Kauai, Hawaii. *US Geological Survey Scientific Investigations Report* 2006–5291.

Jackson, E. D. & Wright, T. L. (1970). Xenoliths in the Honolulu volcanic series, Hawaii. *Journal of Petrology* **11**, 405–430.

Janney, P. E., Le Roex, A. P. & Carlson, R. W. (2005). Hafnium isotope and trace element constraints on the nature of mantle heterogeneity beneath the Central Southwest Indian Ridge (13°E to 47°E). *Journal of Petrology* **46(12)**, 2427–2464, doi:10.1093/petrology/egi060.

Kempton, P. D., Pearce, J. A., Barry, T. L., Fitton, J. G., Langmuir, C. H. & Christie, D. M. (2002). Sr–Nd–Pb–Hf isotope results from ODP Leg 187: Evidence for mantle dynamics of the Australian–Antarctic Discordance and origin of the Indian MORB source. *Geochemistry, Geophysics, Geosystems* **3(12)**, 1074, doi:10.1029/2002GC000320.

Kennedy, A. K., Kwon, S.-T., Frey, F. A. & West, H. B. (1991). The isotopic composition of postshield lavas from Mauna Kea volcano, Hawaii. *Earth and Planetary Science Letters* **103**, 339–353.

Kinzler, R. J. & Grove, T. L. (1992). Primary magmas of mid-ocean ridge basalts 1. Experiments and methods. *Journal of Geophysical Research* **97(B5)**, 6885–6906.

Kurz, M. D., Jenkins, W. J., Hart, S. & Clague, D. (1983). Helium isotopic variations in Loihi Seamount and the island of Hawaii. *Earth and Planetary Science Letters* **66**, 388–406.

Lanphere, M. A. & Frey, F. A. (1987). Geochemical evolution of Kohala Volcano, Hawaii. *Contributions to Mineralogy and Petrology* **95**, 100–113.

Larson, L. M. & Pederson, A. K. (2000). Processes in high-Mg, high T magmas: evidence from olivine, chromite and glass in Paleogene picrites from West Greenland. *Journal of Petrology* **41**, 1071–1098.

Lassiter, J. C. & Hauri, E. H. (1998). Osmium-isotope variations in Hawaiian lavas: evidence for recycled oceanic lithosphere in the Hawaiian plume. *Earth and Planetary Science Letters* **164**, 483–496.

Lassiter, J. C., DePaolo, D. J. & Tatsumoto, M. (1996). Isotopic evolution of Mauna Kea volcano: results from the initial phase of the Hawaiian Scientific Drilling Project. *Journal of Geophysical Research* **101**, 11769–11780.

Lassiter, J. C., Hauri, E. H., Reiners, P. W. & Garcia, M. O. (2000). Generation of Hawaiian post-erosional lavas by melting of mixed lherzolite/pyroxenite source. *Earth and Planetary Science Letters* **178**, 269–284.

Leeman, W. P., Gerlach, D. C., Garcia, M. O. & West, H. B. (1994). Geochemical variations in lavas from Kaho'olawe Volcano, Hawaii; evidence for open system evolution of plume-derived magmas. *Contributions to Mineralogy and Petrology* **116**, 62–77.

Longhi, J. (2002). Some phase equilibrium systematics of lherzolite melting: I. *Geochemistry, Geophysics, Geosystems* **3(3)**, doi:10.1029/2001GC000204.

Lundstrom, C. C., Hoernle, K. & Gill, J. (2003). U-series disequilibria in volcanic rocks from the Canary Islands: Plume versus lithospheric melting. *Geochimica et Cosmochica Acta* **67**, 4153–4177.

Maaløe, S., Tumyr, O. & James, D. (1989). Population density and zoning of olivine phenocrysts in tholeiites from Kauai, Hawaii. *Journal of Petrology* **33**, 761–784.

Maaløe, S., James, D., Smedley, P., Petersen, S. & Garmann, L. B. (1992). The Kōloa Volcanics Suite of Kaua'i, Hawaii. *Journal of Petrology* **33**, 761–784.

Macdonald, G. A. & Katsura, T. (1964). Chemical composition of the Hawaiian lavas. *Journal of Petrology* **5**, 82–133.

Macdonald, G. A., Davis, D. A. & Cox, D. C. (1960). Geology and groundwater resources of the island of Kauai, Hawaii. *Hawai'i Division of Hydrography Bulletin* **13.**

Macdonald, G. A., Abbott, A. T. & Peterson, F. L. (1983). *Volcanoes in the Sea: The Geology of Hawaii.* Honolulu: University of Hawaii Press.

Mahoney, J., LeRoex, A. P., Peng, Z., Fisher, R. L. & Natland, J. H. (1992). Southwestern limits of Indian Ocean ridge mantle and the origin of low $^{206}Pb/^{204}Pb$ mid-ocean ridge basalt: Isotope systematics of the Central Southwest Indian Ridge (17°–50°E). *Journal of Geophysical Research* **97(B13)**, 19771–19790.

Mahoney, J. J., Sinton, J. M., Kurz, M. D., MacDougall, J. D., Spencer, K. J. & Lugmair, G. W. (1994). Isotope and trace element characteristics of a super-fast spreading ridge: East Pacific Rise, 13–23°S. *Earth and Planetary Science Letters* **121**, 173–193.

Marske, J. P., Pietruszka, A. J., Weis, D., Garcia, M. O. & Rhodes, J. M. (2007). Rapid passage of a small-scale mantle heterogeneity through the melting regions of Kīlauea and Mauna Loa volcanoes. *Earth and Planetary Science Letters* **259**, 34–50.

Marske, J. P., Garcia, M. O., Pietruszka, A. P., Rhodes, J. M. & Norman, M. D. (2008). Geochemical variations during Kīlauea's Puu Oo eruption reveal a fine-scale mixture of mantle heterogeneities within the Hawaiian plume. *Journal of Petrology* **49**, 1297–1318.

Matsumoto, A. & Kobayashi, T. (1995). K–Ar age determination of late Quaternary volcanic rocks using the 'mass fractionation correction procedure': application to the Younger Ontake Volcano, central Japan. *Chemical Geology* **125**, 123–135.

Matsumoto, A., Uto, K. & Shibata, K. (1989). K–Ar dating by peak comparison method—New technique applicable to rocks younger than 0·5 Ma. *Bulletin Geological Survey of Japan* **40**, 565–579.

McDonough, W. F. & Sun, S.-s. (1995). The composition of the Earth. *Chemical Geology* **120**, 223–253.

McDougall, I. (1964). Potassium–argon ages from lavas of the Hawaiian Islands. *Geological Society of America Bulletin* **75**, 107–128.

McDougall, I. (1979). Age of shield-building volcanism of Kauai and linear migration of volcanism in the Hawaiian island chain. *Earth and Planetary Science Letters* **46**, 31–42.

Monroe, J. S. & Wicander, R. (1997). *Physical Geology: Exploring the Earth*, 3rd edn. Belmont, CA: Wadsworth Earth Science Series, pp. 34–35.

Mukhopadhyay, S., Lassiter, J. C., Farley, K. A. & Bogue, S. W. (2003). Geochemistry of Kaua'i shield-stage lavas: Implications for the chemical evolution of the Hawaiian plume. *Geochemistry, Geophysics, Geosystems* **4**, 2002GC000342.

Nobre Silva, I. G., Weis, D., Barling, J. & Scoates, J. S. (2009). Leaching systematics and matrix elimination for the determination of high-precision Pb isotope compositions of ocean island basalts. *Geochemistry, Geophysics, Geosystems* **10**, 2009GC002537.

Niu, Y., Collerson, K. D., Batiza, R., Wendt, J. I. & Regelous, M. (1999). Origin of enriched-type mid-ocean ridge basalt at ridges far from mantle plumes: The East Pacific Rise at 11°20′N. *Journal of Geophysical Research* **104**, 7067–7088.

Nowell, G. M., Kempton, P. D., Noble, S. R., Fitton, J. G., Saunders, A., Mahoney, J. J. & Taylor, R. N. (1998). High precision Hf isotope measurements of MORB and OIB by thermal

ionisation mass spectrometry: insights into the depleted mantle. *Chemical Geology* **149**, 211–233.

Ozawa, A., Tagami, T. & Garcia, M. O. (2005). Unspiked K–Ar ages of Honolulu rejuvenated and Koolau shield volcanism on Oahu, Hawaii. *Earth and Planetary Science Letters* **232**, 1–11.

Paul, D., White, W. M. & Blichert-Toft, J. (2005). Geochemistry of Mauritius and the origin of rejuvenescent volcanism on ocean island volcanoes. *Geochemistry, Geophysics, Geosystems* **6**, 2004GC000883.

Pretorius, W., Weis, D., Williams, G., Hanano, D., Kieffer, B. & Scoates, J. (2006). Complete trace elemental characterisation of granitoid (USGS G-2, GSP-2) reference materials by high resolution inductively coupled plasma-mass spectrometry. *Geostandards and Geoanalytical Research* **30**, 39–54.

Putirka, K. D. (2005). Mantle potential temperatures at Hawaii, Iceland, and the mid-ocean ridge system, as inferred from olivine phenocrysts: Evidence for thermally driven mantle plumes. *Geochemistry, Geophysics, Geosystems* **6(Q05L08)**, doi:10.1029/2005GC000915.

Putirka, K. D., Perfit, M. & Ryerson, F. J. (2007). Ambient and excess mantle temperatures, olivine thermometry, and active vs passive upwelling. *Chemical Geology* **241(3–4)**, 177–206, doi:10.1016/j.chemgeo.2007.01.014.

Reiners, P. W. & Nelson, B. K. (1998). Temporal–compositional–isotopic trends in rejuvenated-stage magmas of Kauai, Hawaii, and implications for mantle melting processes. *Geochimica et Cosmochimica Acta* **62**, 2347–2368.

Reiners, P. W., Nelson, B. K. & Izuka, S. K. (1999). Geologic and petrologic evolution of the Lihue Basin and eastern Kauai, Hawaii. *Geological Society of America Bulletin* **111**, 674–685.

Ren, Z.-Y., Ingle, S. S., Takahashi, E., Hirano, N. & Hirata, T. (2005). The chemical structure of the Hawaiian mantle plume. *Nature* **436**, 837–840.

Ren, Z.-Y., Shibata, T., Yoshikawa, M., Johnson, K. & Takahashi, E. (2006). Isotope compositions of submarine Hana Ridge lavas, Haleakala Volcano, Hawaii: Implications for source compositions, melting process and the structure of the Hawaiian plume. *Journal of Petrology* **47**, 255–275.

Ren, Z.-Y., Hanyu, T., Miyazaki, T., Chang, Q., Takahashi, T., Hireahara, Y., Nichols, A. R. L. & Tatsumi, Y. (2009). Geochemical differences of the Hawaiian shield lavas: Implications for melting processes in the heterogeneous Hawaiian plume. *Journal of Petrology* **50**, 1553–1573, doi:10.1093/petrology/egp041.

Rhodes, J. M. (1996). Geochemical stratigraphy of lava flows sampled by the Hawaii Scientific Drilling Project. *Journal of Geophysical Research* **101**, 11729–11746.

Rhodes, J. M. & Vollinger, M. J. (2004). Composition of basaltic lavas sampled by phase-2 of the Hawaii Scientific Drilling Project: Geochemical stratigraphy and magma types. *Geochemistry, Geophysics, Geosystems* **5**, 1–38.

Ribe, N. M. & Christensen, U. R. (1999). The dynamical origin of Hawaiian volcanism. *Earth and Planetary Science Letters* **171**, 517–531.

Robinson, J. E. & Eakins, B. W. (2006). Calculated volumes of individual shield volcanoes at the young end of the Hawaiian ridge. *Journal of Volcanology and Geothermal Research* **151**, 309–317.

Roden, M. F., Trull, T., Hart, S. R. & Frey, F. A. (1994). New He, Nd, Pb, and Sr isotopic constraints on the constitution of the Hawaiian plume: Results from Ko'olau volcano, Oahu, Hawaii. *Earth and Planetary Science Letters* **58**, 1431–158.

Ross, C. S., Foster, M. D. & Meyers, A. T. (1954). Origin of dunites and of olivine-rich inclusions in basaltic rocks. *American Mineralogist* **39**, 693–737.

Salters, V. J. M. (1996). The generation of mid-ocean ridge basalts from the Hf and Nd isotope perspective. *Earth and Planetary Science Letters* **141**, 109–123.

Salters, V. J. M. & Stracke, A. (2004). Composition of the depleted mantle. *Geochemistry, Geophysics, Geosystems* **5(Q05B07)**, doi:10.1029/2003GC000597.

Salters, V. J. & White, W. (1998). Hf isotope constraints on mantle evolution. *Chemical Geology* **145**, 447–460.

Salters, V. J. M., Blichert-Toft, J., Sachi-Kocher, A., Fekiacova, Z. & Bizimis, M. (2006). Isotope and trace element evidence for depleted lithosphere being sampled by the enriched Ko'olau basalts. *Contributions to Mineralogy and Petrology* **151**, 297–312.

Shaw, D. M. (2000). Continuous (dynamic) melting theory revisited. *Canadian Mineralogist* **38(5)**, 1041–1063.

Sherrod, D. R., Sinton, J. M., Watkins, S. E. & Brunt, K. M (2007). Geologic map of the State of Hawaii. *US Geological Survey Open-File Report*, **2007-1089.**

Silva, L. C., Le Bas, M. J. & Robertson, A. H. F. (1981). An oceanic carbonatite volcano on Santiago, Cape Verde Islands. *Nature* **294**, 644–645.

Spengler, S. & Garcia, M. O. (1988). Geochemical evolution of Hawi Formation lavas, Kohala Volcano, Hawaii: The hawaiite to trachyte transition. *Contributions to Mineralogy and Petrology* **99**, 90–104.

Staudigel, H., Zindler, A., Hart, S. R., Leslie, T., Chen, C.-Y. & Clague, D. A. (1984). The isotopic systematics of a juvenile intra-plate volcano: Pb, Nd, and Sr isotope ratios of basalts from Loihi Seamount. *Earth and Planetary Science Letters* **69**, 13–29.

Stearns, H. T. (1947). Geology and groundwater resources of the island of Niihau, Hawaii. *Hawaii Division of Hydrology Bulletin* **12**, 106 pp.

Stearns, H. T. (1946). Geology of the state of Hawaii. *Hawaii Division of Hydrology Bulletin* **8**, 53 pp.

Stearns, H. T. & Vaksvik, K. N. (1935). Geology and groundwater resources of the island of Oahu, Hawaii. *Hawaii Division of Hydrology Bulletin* **1**, 479 pp.

Steiger, R. H. & Jäger, E. (1977). Subcommission on geochronology: convention on the use of decay constants in geo- and cosmochronology. *Earth and Planetary Science Letters* **36**, 359–362.

Stille, P., Unruh, D. M. & Tatsumoto, M. (1983). Pb, Sr, Nd and Hf isotopic evidence of multiple sources for Oahu, Hawaii basalts. *Nature* **304**, 25–29.

Stille, P., Unruh, D. M. & Tatsumoto, M. (1986). Pb, Sr, Nd and Hf isotopic constraints on the origin of Hawaiian basalts and evidence for a unique mantle source. *Geochimica et Cosmochimica Acta* **50**, 2303–2319.

Stracke, A., Salters, V. & Sims, K. (1999). Assessing the presence of garnet-pyroxenite in the mantle sources of basalts through combined hafnium–neodymium–thorium isotope systematics. *Geochemistry, Geophysics, Geosystems* **1**, 1999GC000013.

Tagami, T., Nishimitsu, Y. & Sherrod, D. R. (2003). Rejuvenated-stage volcanism after 0·6-m.y. quiescence at West Maui volcano, Hawaii: new evidence from K–Ar ages and chemistry of Lahaina Volcanics. *Journal of Volcanology and Geothermal Research* **120**, 207–214.

Tanaka, R. & Nakamura, E. (2005). Boron isotopic constraints on the source of Hawaiian shield lavas. *Geochimica et Cosmochimica Acta* **69**, 3385–3399.

Tanaka, R., Nakamura, E. & Takahashi, E. (2002). Geochemical evolution of Koolau volcano. In: Takahashi, E., Lipman, P. W., Garcia, M. O., Naka, J. & Aramaki, S. (eds) *Hawaiian Volcanoes: Deep Underwater Perspectives. American Geophysical Union, Geophysical Monograph* **128**, 311–332.

Tanaka, R., Makishima, A. & Nakamura, E. (2008). Hawaiian double volcanic chain triggered by an episodic involvement of recycled

material: Constraints from temporal Sr–Nd–Hf–Pb isotopic trend of the Loa-type volcanoes. *Earth and Planetary Science Letters* **265**, 450–465.

Tatsumoto, M. (1978). Isotopic composition of lead in oceanic basalt and its implication to mantle evolution. *Earth and Planetary Science Letters* **38**, 63–87.

Walker, G. P. L. (1990). Geology and volcanology of the Hawaiian Islands. *Pacific Science* **44**, 315–347.

Walter, M. J. (1998). Melting of garnet peridotite and the origin of komatiite and depleted lithosphere. *Journal of Petrology* **39**, 29–60.

Wanless, V. D., Garcia, M. O., Rhodes, J. M., Weis, D. & Norman, M. D. (2006). Shield-stage alkalic volcanism on Mauna Loa Volcano, Hawaii. *Journal of Volcanology and Geothemal Research* **151**, 141–155.

Weis, D. & Frey, F. A. (1991). Isotopic geochemistry of Ninetyeast Ridge basement basalts: Sr, Nd and Pb evidence for involvement of the Kerguelen hot spot. In: Weissel, J., Pierce, J., Taylor, E. & Alt, J. (eds) *Proceedings of the Ocean Drilling Program, Scientific Results, 121*. College Station, TX: Ocean Drilling Program, pp. 591–610.

Weis, D. & Frey, F. A. (1996). Role of the Kerguelen plume in generating the eastern Indian Ocean seafloor. *Journal of Geophysical Research* **101**, 13381–13849.

Weis, D., Frey, F. A., Giret, A. & Cantagrel, J. M. (1998). Geochemical characteristics of youngest volcano (Mount Ross) in the Kerguelen Archipelago; inferences for magmaflux, lithosphere assimilation and composition of the Kerguelen Plume. *Journal of Petrology* **39**, 973–994.

Weis, D., Kieffer, B., Maerschalk, C., Pretorius, W. & Barling, J. (2005). High-precision Pb–Sr–Nd–Hf isotopic characterization of USGS BHVO-1 and BHVO-2 reference materials. *Geochemistry, Geophysics, Geosystems* **6**, 2004GC000852.

Weis, D., Kieffer, B., Maerschalk, C., Barling, J., de Jong, J., Williams, G. A., Hanano, D., Pretorius, W., Mattielli, N., Scoates, J. S., Goolaerts, A., Friedman, R. M. & Mahoney, J. B. (2006). High-precision isotopic characterization of USGS reference materials by TIMS and MC-ICP-MS. *Geochemistry, Geophysics, Geosystems* **7**, 2006GC001283.

Weis, D., Kieffer, B., Hanano, D., Nobre Silva, I., Barling, J., Pretorius, W., Maerschalk, C. & Mattielli, N. (2007). Hf isotope compositions of U.S. Geological Survey reference materials. *Geochemistry, Geophysics, Geosystems* **8**, 2006GC001473.

West, H., Gerlach, D., Leeman, W. & Garcia, M. O. (1987). Isotopic constraints on the origin of Hawaiian lavas from the Maui Volcanic Complex, Hawaii. *Nature* **330**, 216–220.

West, H., Garcia, M. O., Frey, F. & Kennedy, A. (1988). Evolution of alkalic cap lavas, Mauna Kea Volcano, Hawaii. *Contributions to Mineralogy and Petrology* **100**, 383–397.

White, R. W. (1966). Ultramafic inclusions in basaltic rocks from Hawaii. *Contributions to Mineralogy and Petrology* **12**, 245–314.

Woods, M. T., Leveque, J.-J., Okal, E. A. & Cara, M. (1991). Two station measurements of Rayleigh wave group velocity along the Hawaiian swell. *Geophysical Research Letters* **18**, 105–108.

Wright, E. & White, W. M. (1987). The origin of Samoa; new evidence from Sr, Nd, and Pb isotopes. *Earth and Planetary Science Letters* **81**, 151–162.

Wright, T. L. (1971). Chemistry of Kīlauea and Mauna Loa lava in space and time. US Geological Survey Professional Paper **735**, 1–45.

Xu, G., Frey, F. A., Clague, D. A., Weis, D. & Beeson, M. H. (2005). East Molokai and other Kea-trend volcanoes: Magmatic processes and sources as they migrate away from the Hawaiian hot spot. *Geochemistry, Geophysics, Geosystems* **6**, 2004GC000830.

Xu, G., Frey, F. A., Clague, D. A., Abouchami, W., Blichert-Toft, J., Cousens, B. & Weisler, M. (2007). Geochemical characteristics of West Molokai shield- and postshield-stage lavas: Constraints on Hawaiian plume models. *Geochemistry, Geophysics, Geosystems* **8**, 2006GC001554.

Yang, H. J., Frey, F. A. & Clague, D. A. (2003). Constraints on the source components of lavas forming the Hawaiian North Arch and Honolulu Volcanics. *Journal of Petrology* **44**, 603–627.

Zou, H. & Reid, M. R. (2001). Quantitative modeling of trace element fractionation during incongruent dynamic melting. *Geochimica et Cosmochimica Acta* **65**, 153–162.